STRESSES AND DISPLACEMENTS IN A THICK LAYER CONTAINING AN AXIALLY SYMMETRICAL DUGDALE CRACK

A Thesis

Presented to

the Faculty of the Department of Mechanical Engineering

University of Houston

In Partial Fulfillment

of the Requirements for the Degree

Master of Science in Mechanical Engineering

---

by

John Russell Shadley

June , 1968

ACKNOWLEDGMENTS

The author would like to express his appreciation and thanks to the following:

Dr. Z. Olesiak, Visiting Professor of Mechanical Engineering, for suggesting the thesis topic and for his continued advice and assistance throughout the course of this investigation;

The National Science Foundation for the financial assistance which made this investigation possible;

Mrs. Marjorie Carroll for typing the manuscript.

STRESSES AND DISPLACEMENTS IN A THICK LAYER CONTAINING AN AXIALLY SYMMETRICAL DUGDALE CRACK

An Abstract of a Thesis

Presented to

the Faculty of the Department of Mechanical Engineering

University of Houston

In Partial Fulfillment

of the Requirements for the Degree

Master of Science in Mechanical Engineering

---

by

John Russell Shadley

June , 1968

ABSTRACT

Presented in this thesis is an analytical solution to the problem of the determination of stresses and displacements in a layer of elastic-perfectly plastic material containing a penny-shaped crack. It is assumed that the zone of plastic deformations surrounding the crack is very thin so that the problem can be reduced to one, within the theory of elasticity, of determining the stresses and displacements in an elastic half-layer with proper boundary conditions.

Through the application of Hankel transforms, the problem is reduced to that of solving a pair of dual-integral equations. The dual-integral equations are solved by reducing them to a Fredholm integral equation of the second kind. The integral equation is then solved by numerical methods.

The width of the annulus of yielded material is determined from the condition that the stress at the crack tips must be finite. The stresses and displacements on the plane of symmetry are then computed by numerical integration of the inverse Hankel transforms.

Numerical examples are tabulated and plotted for plastic zone widths, stresses, and displacements corresponding to various layer thicknesses and loading pressures. The results are discussed regarding their relation to the case of an infinite body, and regarding the applicability of the assumptions of small strains and thin yield zones.

TABLE OF CONTENTS

LIST OF SYMBOLS

a	plastic zone radius, radius of crack plus width of plastic zone
h	half-thickness of layer
ℓ	radius of crack
p	dimensionless ratio of plastic zone radius to half-thickness of layer, a/h
p(r)	pressure distribution on crack surface
q	uniform loading pressure on crack surface
r	radial coordinate measured from axis of symmetry
u	r-component of displacement vector
w	z-component of displacement vector
Y	yield limit of material
z	axial coordinate measured from plane of symmetry
γ	dimensionless ratio of loading pressure to yield limit, q/Y
δ	dimensionless ratio of crack radius to plastic zone radius, ℓ/a
μ	shear modulus
ν	Poisson's ratio
ρ	dimensionless coordinate, r/a

LIST OF FIGURES

LIST OF TABLES

CHAPTER I

INTRODUCTION

1. Bibliographical Remarks

The study of equilibrium cracks concerns the study of the equilibrium of solids in the presence of cracks. The objectives of such studies are to determine the stress field around a crack, the displacements of the crack faces, and eventually, information relating the mechanism of fracture to certain parameters such as initial crack size, the shape, size, and material characteristics of the solid, and the loading configuration on the solid.

The methods of investigation of an elastic body containing cracks differ from those used in the case of solids with cavities. Usually the displacements and angular changes of the surfaces of a cavity in a solid are small and can, therefore, be determined by the classical linear theory of elasticity. In crack theory, however, angular changes may be large, and the crack boundary may expand considerably even when the body containing the crack is subjected to a small increase in load. The determination of the boundary, in fact, becomes part of the problem.

Comprehensive review articles on the theory of cracks have been published by G. R. Irwin [1][1], G. I. Barenblatt [2],

---

[1] Numbers in brackets refer to references listed in the Bibliography.

P. C. Paris and G. C. Sih [3], and I. N. Sneddon [4]. These papers contain a general survey of the development of crack theory with references to numerous original papers. It is the purpose of this introduction to acquaint the reader with a few of the most important developments in the theory of cracks and certain papers that led in a direct way to the solution of the problem presented in this thesis.

Although a solution to the crack problem can be found by applying the differential equations of equilibrium and the usual boundary to a solid with an elliptical cavity, the solution is not entirely satisfactory. C. E. Inglis [5] in 1913 presented a solution of an infinite two-dimensional elastic space containing an elliptical cavity, where the crack was taken to be an ellipse of zero minor axis. Since that time, authors including Muskhelishvili [6], Westergaard [7], Sneddon [8], who introduced the application of Fourier transforms to the solution of equilibrium crack problems, and many others have obtained solutions to various problems in equilibrium crack theory by considering the crack to be an elliptical cavity in an elastic solid. In every such solution, however, the stress normal to the surface of the crack is infinite at the crack tips, the shape of the crack surfaces at the tips appears unnaturally rounded, and although experience would suggest that the length of the crack is very much dependent upon the applied load, a solution corresponding to a particular applied load may be constructed for any arbitrarily selected crack length.

It was an important idea first advanced by A. A. Griffith [9] in 1920 that sparked further efforts in the theory of cracks. Griffith suggested that in a brittle body, molecular forces of cohesion, acting between the crack faces near the edge of the crack where the distance between the opposite faces is very small, influenced greatly the mechanism of fracture of the brittle body. To cause a crack to extend, work must be done against these cohesive forces on either side of the crack. The energy per unit area of newly created crack surface was termed by Griffith the "surface tension" of the material. By considering the region at the crack tips influenced by these cohesive forces to be very small, Griffith was able to calculate the critical value, p_o, of a uniform stress applied to the boundary of an infinite brittle body with a straight line crack that would cause the crack to extend.

S. A. Khristianovitch [10] in 1955 hit upon an idea which helped resolve the problem of indefiniteness of crack length. In connection with studying hydraulic fracture in an oil-bearing stratum, he considered the problem of an infinite body containing an isolated crack. The material surrounding the crack was subjected to constant compressive stresses due to the weight of the rock above, and the crack surfaces were compressed by a uniformly distributed pressure due to the fluid inside the crack. Khristianovitch found that when his model allowed the fluid to fill the crack completely, the tensile stresses at the crack tips were infinite. But, when the fluid filled the crack only partially, so that the crack faces near the tips were free of stress, one exceptional value of the crack length could be found that would cause the resulting stresses at the crack tips to be finite.

Based on this observation of Khristianovitch, Barenblatt [1, 11] advanced the hypothesis that the condition of finiteness of stress is fundamental in the determination of crack length, and that it is identical with the condition of smooth closing of the opposite faces of a crack at its edges into a cusp. He was able to satisfy this condition by considering the influence of the molecular forces of cohesion at the crack tips on stress and displacement.

Further interest in crack theory developed following the publication of papers by G. R. Irwin [12] and E. O. Orowan [13] concerning the concept of the "quasi-brittle"[2] fracture. They observed that certain materials, which normally exhibit highly ductile behavior in standard tensile tests, fracture

---

[2] This term is rather misleading because it suggests that a "quasi-brittle" solid behaves nearly like a brittle one. In fact, the situation encountered in experiment is the opposite. In the work done by Gerberich [14] and Swedlow and Gerberich [15] it was demonstrated that only very ductile materials, for example low carbon steels or certain aluminum alloys, exhibit the highly localized plastic zones preceding the crack tips. Thus, according to the accepted terminology, they are "quasi-brittle," while the harder materials, which show work-hardening effect, are not "quasi-brittle."

in a way similar to the behavior of brittle materials when cracks are forming. This behavior suggests that the arising plastic deformations are concentrated in a very narrow layer at the crack surface. In such cases Irwin and Orowan were able to apply Griffith's theory of brittle fracture where the work required to produce plastic deformations at the crack surface is added to (or replaces, if large enough) the work, in Griffith's model, required to overcome the molecular forces of cohesion.

While investigating the static yielding at the ends of slits in stretched plates, N. E. Frost and D. S. Dugdale [16] noticed that the yielded zones were thin extensions of the crack lines.[3] Dugdale [17] then suggested that in an elastic-perfectly plastic material of yield limit, Y, the sheet may be considered to deform elastically under the action of the external stress together with a uniform tensile stress, Y, distributed over part of the surface of a hypothetical cut of length 2a, where 2ℓ is the actual crack length and $a-\ell$ is the width of the plastic zone. Such a crack has become known as a "Dugdale Crack."

Utilizing the observations of Frost and Dugdale, J. N. Goodier and F. A. Field [20] applied the methods of elastic-perfectly plastic continuum mechanics to the two-dimensional

---

[3] For a discussion of stresses in materials where the yielded zones are not simply thin extensions of the crack lines, see papers by J. R. Rice [18] and F. A. McClintock and G. R. Irwin [19].

problem of an infinite plate of elastic-perfectly plastic material containing a crack, and calculated the plastic energy dissipation associated with propagation of the crack.

Publications that led in a direct way to the solution to the problem presented in this thesis include those of Z. Olesiak and M. Wnuk [21,22], Ya. S. Uflyand [23], and L. M. Keer [24]. Olesiak and Wnuk treated the problem of an elastic-perfectly plastic infinite medium containing a disc-shaped ("penny-shaped") crack. Using the concept of Barenblatt that no infinite stresses may exist at the crack tips, and extending the hypothesis of Dugdale to the case of axial symmetry, they applied Hankel integral transforms to the equations of equilibrium to find the width of the annulus of yielded material around the crack. Later they extended the problem to evaluate displacements of the crack surfaces, and to compute the plastic energy dissipation and the critical applied pressure associated with extension of the crack.

Through the use of potential functions, Uflyand and Keer solved the problem of determining the stresses and displacements in a thick, elastic plate containing a penny-shaped cavity. They reduced the problem to that of determining an auxiliary function satisfying a Fredholm integral equation. Uflyand solved for the auxiliary function by numerical methods and presented the function solution in tabulated form.

2. Definition of the Problem

Treated in this thesis is the problem of a layer of elastic-perfectly plastic material containing a penny-shaped crack. The purpose is to determine the width of the annulus of yielded material around the crack, the stresses in the elastic material outside the plastic zone on the plane of symmetry, and the displacements of the crack faces when the boundaries of the layer are free of stress except for a uniform pressure on the crack faces.

By applying an appropriate fracture criterion to the stress and displacement data computed in this thesis, the problem can be extended to that of determining conditions of geometry and loading that will cause the crack to extend and eventually fail the material in fracture.

CHAPTER II

ANALYTICAL SOLUTION OF THE TITLE PROBLEM

1. Description of the Model

The model applied to this problem is shown in Figure 1. The axially symmetrical crack of radius lies in the plane of symmetry of an infinite layer of meterial of thickness 2h. It is assumed, in accordance with Dugdale's observation concerning the behavior of thin plates, that the solid is elastic except for a very thin annulus of plastically deformed material surrounding the crack. The width of the annulus, a-λ, is such that no stress singularity occurs at the tip of the elastic-plastic interface.

The non-zero components of the stress tensor σ_r, σ_θ σ_z, τ_{rz} are required to satisfy the Huber-Mises-Henky plasticity condition in the yielded zone. But if it is assumed that the material is elastic-perfectly plastic and all stress components in the plastic zone are small compared with σ_z, the plasticity condition is approximately satisfied if it is assumed that σ_z equals a constant, Y, in this region, where Y denotes the stress at which yielding begins in the simple tensile test. The only loading to be considered on the layer is a uniform pressure, q, on the crack faces.

By the above assumptions, the problem can be reduced to the problem, within the theory of elasticity, of finding the

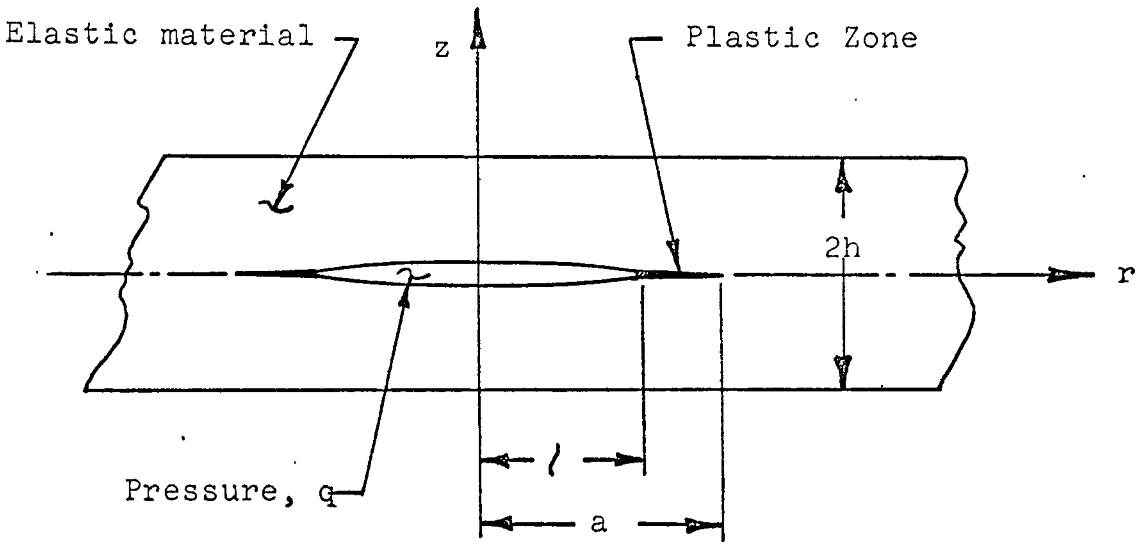

FIGURE 1
CRACK MODEL

stresses and displacements in one half the layer, Figure 2, with the following boundary conditions:

for z=0 (1)

$$\tau_{rz} = 0, \quad r \geq 0$$

$$\sigma_z = -p(r) = \begin{cases} -q, & 0 \leq r < l \\ +y, & l < r < a \end{cases}$$

$$w = 0, \quad r > a$$

for z=h (2)

$$\tau_{rz} = 0, \quad r \geq 0$$

$$\sigma_z = 0, \quad r \geq 0$$

where τ_{rz} is the shear stress in the r,z-plane, σ_z is the normal stress in the z direction, and w is the z-component of the displacement vector.

2. Reduction of the Problem to the Dual-Integral Equations

Since the geometry of the problem is symmetrical about the z-axis, the equations of equilibrium can be written as Navier's equations in cylindrical coordinates for axial symmetry,

$$2(1-\nu)\left(\frac{\partial^2 u}{\partial r^2} + \frac{1}{r}\frac{\partial u}{\partial r} - \frac{u}{r^2}\right) + (1-2\nu)\frac{\partial^2 u}{\partial z^2} + \frac{\partial^2 w}{\partial r \partial z} = 0 \qquad (3)$$

$$(1-2\nu)\left(\frac{\partial^2 w}{\partial r^2} + \frac{1}{r}\frac{\partial w}{\partial r}\right) + 2(1-\nu)\frac{\partial^2 w}{\partial z^2} + \frac{\partial}{\partial z}\left(\frac{\partial u}{\partial r} + \frac{u}{r}\right) = 0 \qquad (4)$$

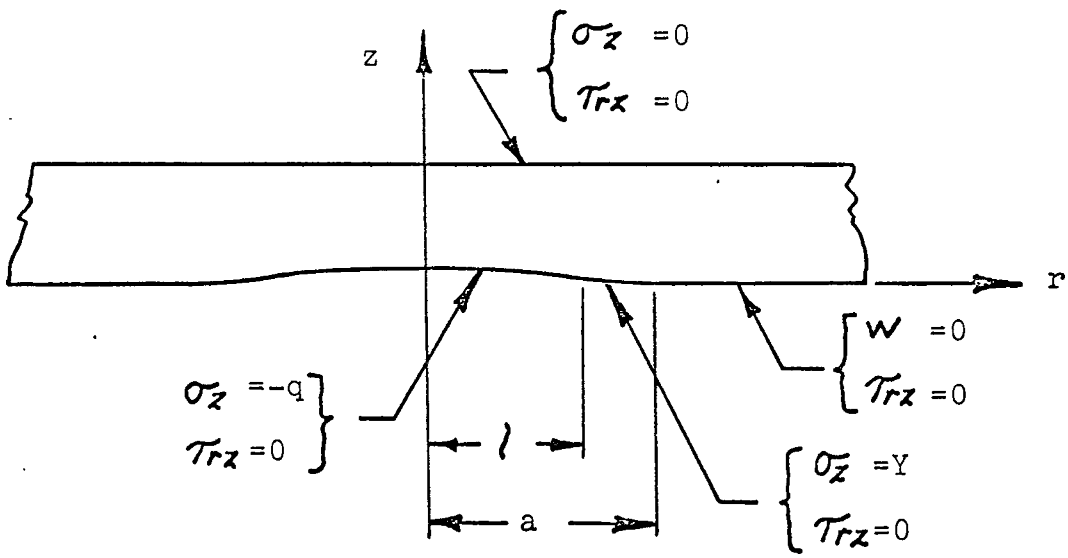

FIGURE 2

BOUNDARY CONDITIONS

where u and w are the components of the displacement vector in the r and z directions and ν is Poisson's ratio.

Following Z. Olesiak and I. N. Sneddon [25], Hankel transforms of the first and zeroth order can be applied by multiplying Eq. (3) by $rJ_1(r\xi)dr$ and Eq. (4) by $rJ_0(r\xi)dr$ and integrating from zero to infinity, yielding the transformed equations

$$[(1-2\nu)D^2-2(1-\nu)\xi^2]\bar{u}-\xi D\bar{w}=0 \tag{5}$$

$$[2(1-\nu)D^2-(1-2\nu)\xi^2]\bar{w}+\xi D\bar{u}=0 \tag{6}$$

where

$$\bar{u}(\xi,z)=\int_0^\infty ru(r,z)J_1(\xi r)dr, \quad \bar{w}(\xi,z)=\int_0^\infty rw(r,z)J_0(\xi r)dr$$

and $$D\equiv\frac{d}{dz}$$

By substituting one into the other, the pair of Eqs. (5) and (6) can be reduced to a more convenient form

$$(D^2-\xi^2)^2\bar{u}=0 \tag{7}$$

$$(D^2-\xi^2)^2\bar{w}=0 \tag{8}$$

The solutions of Eqs. (7) and (8) have the form

$$\bar{u}=(A_1+A_2z\xi)\cosh\xi z+(A_3+A_4z\xi)\sinh\xi z$$

$$\bar{w}=(B_1+B_2z\xi)\cosh\xi z+(B_3+B_4z\xi)\sinh\xi z$$

Since the system of Eqs. (5) and (6) admits four independent constants of integration only, $\bar{u}$ and $\bar{w}$ may now be substituted back into (5) and (6) to find

$$\begin{aligned} A_1 &= -(3-4\nu)B_2 - B_3 \\ A_2 &= -B_4 \\ A_3 &= -(3-4\nu)B_4 - B_1 \\ A_4 &= -B_2 \end{aligned}$$

The solutions for $\bar{u}$ and $\bar{w}$ can now be written

$$\begin{aligned} \bar{u} = &-[(3-4\nu)B_2 + B_3 + B_4 z\xi]\cosh\xi z \\ &-[(3-4\nu)B_4 + B_1 + B_2 z\xi]\sinh\xi z \end{aligned} \tag{9}$$

$$\bar{w} = (B_1 + B_2 z\xi)\cosh\xi z + (B_3 + B_4 z\xi)\sinh\xi z \tag{10}$$

The constants of integration, B_1 through B_4, must be evaluated from the boundary condition (1) on the plane of symmetry, z=0, and the boundary condition (2) on the surface of the layer, z=h.

The expressions for shear stress and the z-component of normal stress in cylindrical coordinates for axial symmetry are

$$\tau_{rz} = \mu\left(\frac{\partial u}{\partial z} + \frac{\partial w}{\partial r}\right)$$

$$\sigma_z = \frac{2\mu}{1-2\nu}\left[(1-\nu)\frac{\partial w}{\partial z} + \nu\left(\frac{\partial u}{\partial r} + \frac{u}{r}\right)\right]$$

where μ is the shear modulus. As shown by Z. Olesiak and I. N. Sneddon [25] the Hankel transforms of these equations are as follows:

$$\bar{\tau}_{rz} = \mu (D\bar{u} - \xi \bar{w})$$

$$\bar{\sigma}_z = \frac{2\mu}{1-2\nu}\left[(1-\nu)D\bar{w} + \nu \xi \bar{u}\right]$$

where

$$\bar{\tau}(\xi,z) = \int_0^\infty r\tau(r,z)J_1(\xi r)\,dr, \quad \bar{\sigma}(\xi,z) = \int_0^\infty r\sigma(r,z)J_0(\xi z)\,dr$$

By substituting for $\bar{u}$ and $\bar{w}$ from Eqs. (9) and (10), the solutions for $\bar{\tau}$ and $\bar{\sigma}$ can be written

$$\bar{\tau}_{rz} = -2\mu\xi\left\{\left[2(1-\nu)B_2 + B_3 + \xi z B_4\right]\sinh\xi z + \left[2(1-\nu)B_4 + B_1 + \xi z B_2\right]\cosh\xi z\right\} \tag{11}$$

$$\bar{\sigma}_z = 2\mu\xi\left\{\left[(1-2\nu)B_4 + B_1 + \xi z B_2\right]\sinh\xi z + \left[(1-2\nu)B_2 + B_3 + \xi z B_4\right]\cosh\xi z\right\} \tag{12}$$

For the boundary condition

$$\bar{\tau}_{rz} = 0, \qquad \text{on } z=0$$

Eq. (11) yields the relation

$$B_1 = -2(1-\nu)B_4 \tag{13}$$

From (13) and the boundary condition

$$\tau_{rz} = 0 \qquad \text{on } z=h$$

Eq. (11) yields the relation

$$B_3 = -[2(1-\nu)B_2 + \xi h B_4] - \xi h B_2 \frac{\cosh \xi h}{\sinh \xi h} \tag{14}$$

From (13) and the boundary condition

$$\sigma_z = 0 \qquad \text{on } z=h$$

Eq. (12) yields the relation

$$B_3 = -[\xi h B_2 - B_4]\frac{\sinh \xi h}{\cosh \xi h} - [(1-2\nu)B_2 + \xi h B_4]\cosh \xi h \tag{15}$$

After solving Eqs. (14) and (15) for B_2 and B_3, three constants can be written in terms of the fourth,

$$\left.\begin{aligned} B_1 &= -2(1-\nu)B_4 \\ B_2 &= -\frac{\sinh^2 \xi h}{\xi h + \sinh \xi h \cosh \xi h} B_4 \\ B_3 &= \frac{2(1-\nu)\sinh^2 \xi h - \xi^2 h^2}{\xi h + \sinh \xi h \cosh \xi h} B_4 \end{aligned}\right\} \tag{16}$$

The fourth constant must be found from the boundary conditions on the plane z=0, where the z-component of the displacement vector for $r > a$ is equal to zero, and the z-component of the normal stress for $r < a$ is equal to the pressure on the crack surface.

In terms of the constant B_1, Eqs. (10) and (12) on the plane z=0 are

$$\bar{w}_{z=0} = B_1 \tag{17}$$

$$\bar{\sigma}_{z=0} = \frac{\mu}{1-\nu}\left[\frac{\xi^2 h^2 - \sinh^2 \xi h}{\xi h + \sinh \xi h \cosh \xi h}\right]\xi B_1 \tag{18}$$

Hence, the boundary conditions require that on the plane of symmetry

$$w = \int_0^\infty \xi B_1(\xi) J_0(r\xi)\, d\xi = 0\,, \qquad r > a \tag{19}$$

$$\sigma_z = \frac{\mu}{1-\nu}\int_0^\infty \frac{\xi^2 h^2 - \sinh^2 \xi h}{\xi h + \sinh \xi h \cosh \xi h}\, \xi B_1(\xi) J_0(r\xi)\, d\xi = -p(r)\,, \quad 0 \le r < a \tag{20}$$

where the inverse Hankel transforms for w and σ_z on the plane of symmetry are

$$w(r,z) = \int_0^\infty \xi\, \bar{w}(\xi, z) J_0(\xi r)\, d\xi\,, \qquad \sigma_z(r,z) = \int_0^\infty \xi\, \bar{\sigma}_z(\xi, z) J_0(\xi r)\, d\xi$$

The pair of dual-integral equations, (19) and (20), must be solved for the parameter $B_1(\xi)$. The stress tensor and the displacement vector can then be found by computing the inverse Hankel transforms.

A pair of dual-integral equations in agreement with Eqs. (19) and (20) was obtained by Ya. S. Uflyand [23], p.202, through the use of harmonic stress functions.

3. Method of Solving the Dual-Integral Equations by the Reduction to a Fredholm Integral Equation

Following Ya. S. Uflyand [23], p.202, assume that

$$\xi^2 B_1(\xi) = \int_0^a \phi(t)(\cos\xi t - \cos\xi a)\,dt \tag{21}$$

where $\phi(t)$ is a function to be determined that exists in the interval [o,a]. Eqs. (19) and (20) can now be written

$$w_{z=0} = \int_0^\infty \frac{1}{\xi}\int_0^a \phi(t)(\cos\xi t - \cos\xi a)\,dt\, J_0(r\xi)\,d\xi = 0, \quad r > a \tag{22}$$

$$\frac{1-\nu}{\mu}\sigma_{z\,z=0} = \int_0^\infty \frac{\xi^2h^2 - \sinh^2\xi h}{\xi h + \sinh\xi h\cosh\xi h}\int_0^a \phi(t)(\cos\xi t - \cos\xi a)\,dt$$

$$J_0(r\xi)\,d\xi = \frac{-(1-\nu)}{\mu}p(r), \quad 0 \le r < a \tag{23}$$

This choice for the form of the parameter $B_1(\xi)$ satisfies Eq. (22) identically. If the order of integration is changed in Eq. (22) the equation can be written

$$W_{z=0} = \int_0^a \phi(t) \int_0^\infty \frac{(\cos\xi t - \cos\xi a)}{\xi} J_0(r\xi)\, d\xi\, dt = 0 \quad r > a \tag{24}$$

In Olesiak and Sneddon's work [25], the following relation is given

$$\int_0^\infty \frac{1}{\xi}(1-\cos a\xi) J_0(\xi r)\, d\xi = \begin{cases} 0, & r > a \\ \cosh^{-1}\frac{a}{r}, & 0 \le r < a \end{cases} \tag{25}$$

Since in Eq. (24) $t \leq a$ always, the inside integral assumes the values

$$\int_0^\infty \frac{(\cos\xi t - \cos\xi a)}{\xi} J_0(r\xi)\, d\xi = \begin{cases} 0, & r > a \\ \cosh^{-1}\frac{a}{r}, & t < r < a \\ \cosh^{-1}\frac{a}{r} - \cosh^{-1}\frac{t}{r}, & r < t \end{cases} \tag{26}$$

Therefore, $W_{z=0}$ is zero for all $r > a$, and Eq. (22) is satisfied identically.

If, in Eq. (23), the order of integration is interchanged, and since

$$\frac{\xi^2 h^2 - \sinh^2\xi h}{\xi h + \sinh\xi h \cosh\xi h} = g(\xi) - 1$$

where

$$g(\xi) = \frac{\xi h(\xi h + 1) + \sinh\xi h\, e^{-\xi h}}{\xi h + \cosh\xi h \sinh\xi h} \tag{27}$$

Eq. (23), for $0 \leq r < a$ can be written

$$\int_0^a \phi(t)\int_0^\infty (\cos\xi t - \cos\xi a)\, J_0(r\xi)\, d\xi\, dt - \int_0^a \phi(t)\int_0^\infty g(\xi)(\cos\xi t - \cos\xi a) J_0(r\xi)\, d\xi\, dt = \frac{1-\nu}{\mu} p(r) \tag{28}$$

The following definite integral can be found, for example, in Erdélyi [26]:

$$\int_0^\infty \cos\xi t\, J_0(r\xi)\, d\xi = \begin{cases} 0, & t > r \\ 1/\sqrt{r^2 - t^2}, & 0 \leq t < r \end{cases}$$

$$\int_0^\infty \cos\xi a\, J_0(r\xi)\, d\xi = \begin{cases} 0, & a > r \\ 1/\sqrt{r^2 - a^2}, & 0 \leq a < r \end{cases} \tag{29}$$

and since Eq. (28) applies only to the interval $0 \leq r < a$, the first term in Eq. (28) is

$$\int_0^a \phi(t)\int_0^\infty (\cos\xi t - \cos\xi a) J_0(r\xi)\, d\xi\, dt = \int_0^r \frac{\phi(t)\, dt}{\sqrt{r^2 - t^2}}$$

By making use of the relation

$$J_0(\xi r) = \frac{2}{\pi}\int_0^r \cos(\xi x)\, \frac{dx}{\sqrt{r^2 - x^2}} \tag{30}$$

and interchanging the order of integration in the second term of Eq. (28), the equation can be written

$$\int_0^r \frac{\phi(t)\,dt}{\sqrt{r^2-t^2}} - \frac{2}{\pi}\int_0^a \phi(t) \int_0^r \frac{1}{\sqrt{r^2-x^2}} \int_0^\infty g(\xi)(\cos\xi t - \cos\xi a)$$

$$\cos(\xi x)\,d\xi\,dx\,dt = \frac{(1-\nu)}{\mu}p(r) \tag{31}$$

By the use of the trigonometric identities

$$\cos\xi t\cos\xi x = \tfrac{1}{2}[\cos\xi(t+x) + \cos\xi(t-x)]$$

$$\cos\xi a\cos\xi x = \tfrac{1}{2}[\cos\xi(a+x) + \cos\xi(a-x)]$$

a Fourier cosine transform can be defined

$$G(u) = \int_0^\infty g(\xi)\cos\xi u\,d\xi \tag{32}$$

such that Eq. (31) reduces to an integral equation of the Abel type

$$\int_0^r \frac{\phi(t)\,dt}{\sqrt{r^2-t^2}} - \frac{1}{\pi}\int_0^a \phi(t) \int_0^r \frac{1}{\sqrt{r^2-x^2}} K(t,x,a)\,dx\,dt$$

$$= \frac{(1-\nu)}{\mu}p(r) \tag{33}$$

where

$$K(t,x,a) = G(t+x) + G(t-x) - G(a+x) - G(a-x) \tag{34}$$

The above integral equation was reduced by Uflyand to the integral equation of Schloemilch

$$\int_0^{\pi/2} F(r\sin\theta)\,d\theta = f(r), \quad 0 \le r \le a \tag{35}$$

where

$$F(x) = \phi(x) - \frac{1}{\pi}\int_0^a \phi(t)\,K(t,x,a)\,dt, \quad 0 \le x \le a \tag{36}$$

Eq. (34) and Eqs. (35) and (36) were solved for the kernel, $K(t,x,a)$, and the function $\phi(X)$ by numerical methods and tabulated by Ya. S. Uflyand [23], p.204, for the case that $f(r)$ equals a constant.

However, Eq. (33) can be reduced directly to a Fredholm integral equation of the second kind by employing a method also used by Keer [24]. By multiplying the equation by $r/\sqrt{s^2-r^2}$, integrating with respect to r from 0 to s, and differentiating with respect to s, the first term in Eq. (33) becomes

$$\frac{d}{ds}\int_0^s\int_0^r \frac{\phi(t)\,dt}{\sqrt{r^2-t^2}}\,\frac{r\,dr}{\sqrt{s^2-r^2}} = \frac{d}{ds}\int_0^s \phi(t)\int_t^s \frac{r\,dr\,dt}{\sqrt{(r^2-t^2)(s^2-r^2)}} = \frac{\pi}{2}\,\phi(s)$$

and the second term becomes

$$-\frac{1}{\pi}\int_0^a \phi(t)\frac{d}{ds}\int_0^s\int_0^r \frac{K(t,x,a)}{\sqrt{r^2-x^2}}dx\,\frac{r\,dr}{\sqrt{s^2-r^2}}\,dt$$

$$=-\frac{1}{\pi}\int_0^a \phi(t)\frac{d}{ds}\int_0^s\int_x^s \frac{K(t,x,a)\,r\,dr}{\sqrt{(r^2-x^2)(s^2-r^2)}}\,dx\,dt$$

$$=-\frac{1}{2}\int_0^a \phi(t)\,K(t,s,a)\,dt$$

Finally, after defining

$$F(s)=\frac{2}{\pi}\,\frac{(1-\nu)}{\mu}\,\frac{d}{ds}\int_0^s \frac{p(r)\,r}{\sqrt{s^2-r^2}}\,dr \tag{37}$$

and multiplying the whole of Eq. (33) by $2/\pi$, one obtains the following Fredholm integral equation of the second kind:

$$\phi(s)-\frac{1}{\pi}\int_0^a \phi(t)\,K(t,s,a)\,dt=F(s) \tag{38}$$

Given a particular pressure distribution, $p(r)$ on the crack surface, the integral equation (38) can be solved by numerical methods. To this end, the kernel, $K(t,s,a)$ must be computed for values of t and s between 0 and a.

Eq. (38) can then be solved for $\phi(s)$, $0 \le s \le a$. Since the parameter $B_1(\xi)$ is related to $\phi(s)$ by Eq. (21), the stresses and displacements on the plane of symmetry can then be computed by applying the inverse Hankel transforms to Eqs. (17) and (18).

4. Determination of the Width of Plastic Zones

The pressure distribution, $p(r)$, for the circular crack was given in Eq. (1)

$$p(r) = \begin{cases} g, & 0 \le r < l \\ -Y, & l \le r < a \end{cases}$$

Therefore, from the definition of $F(s)$,

$$F(s) = \frac{2}{\pi}\frac{(1-\nu)}{\mu} \begin{cases} g, & s < l \\ g - \frac{s}{\sqrt{s^2-l^2}}(g+Y), & l < s < a \end{cases} \tag{39}$$

In order to perform the numerical calculations on the Fredholm integral equation (38), it is convenient to define dimensionless variables and parameters as follows:

$$\sigma = \frac{s}{a}, \ \tau = \frac{t}{a}, \ \delta = \frac{l}{a}, \ \alpha = h\xi, \ p = \frac{a}{h} \tag{40}$$

The Fourier cosine transform, Eq. (32), can be written

$$aG(u) = p\int_0^\infty \frac{\alpha(1+\alpha)+\sinh\alpha\, e^{-\alpha}}{\alpha+\cosh\alpha\sinh\alpha}\cos(p\alpha u)\,d\alpha \qquad (41)$$

and the kernel of the Fredholm integral equation (34), in dimensionless form, can be written

$$\begin{aligned} aK(a\tau, a\rho) = {} & aG[a(\tau+\rho)] + aG[a(\tau-\rho)] \\ & - aG[a(1+\rho)] - aG[a(1-\rho)] \end{aligned} \qquad (42)$$

where τ and ρ vary between 0 and 1.

Matrices of the quantity $aK(a\tau, a\rho)$ for various values of the parameter, p, are given in Table I, where the transforms, G(u), were evaluated by use of the trapezoidal rule and agree with those tabulated by Ya. S. Uflyand [23], p.204.

If the width of the plastic zone were known, (i.e., if $\delta = l/a$ were fixed) at this point, the integral equation (38) and the problem of determining the stresses and displacements could be solved as shown by Uflyand. Here, however, the width of the plastic zone is not known. The Fredholm integral equation must be solved for a family of solutions for the function $\phi(l, S)$ where l varies incrementally between 0 and a. The stress at the plane z=0 must be computed for each value of l. The width of the plastic zone, a-l, can then be determined from the condition that the stresses must be finite at the crack tips, (i.e., at r=a).

TABLE I

MATRIX OF KERNELS, $aK(a\xi, a\tau)$

p=0.1

ξ	τ=0.0	τ=0.1	τ=0.2	τ=0.3	τ=0.4	τ=0.5
0.0	0.004207	0.004206	0.004201	0.004194	0.004184	0.004170
0.1	0.004165	0.004163	0.004159	0.004152	0.004142	0.004128
0.2	0.004037	0.004036	0.004032	0.004025	0.004015	0.004003
0.3	0.003827	0.003825	0.003821	0.003814	0.003805	0.003793
0.4	0.003531	0.003529	0.003525	0.003520	0.003511	0.003500
0.5	0.003150	0.003149	0.003146	0.003141	0.003133	0.003123
0.6	0.002687	0.002686	0.002683	0.002679	0.002672	0.002664
0.7	0.002139	0.002138	0.002137	0.002133	0.002128	0.002121
0.8	0.001509	0.001508	0.001507	0.001504	0.001501	0.001496
0.9	0.000796	0.000795	0.000794	0.000793	0.000791	0.000789
1.0	0.000000	0.000000	0.000000	0.000000	0.000000	0.000000

ξ	τ=0.6	τ=0.7	τ=0.8	τ=0.9	τ=1.0
0.0	0.004154	0.004135	0.004114	0.004090	0.004063
0.1	0.004112	0.004093	0.004072	0.004048	0.004022
0.2	0.003987	0.003969	0.003948	0.003925	0.003899
0.3	0.003779	0.003761	0.003742	0.003719	0.003695
0.4	0.003486	0.003470	0.003452	0.003432	0.003410
0.5	0.003111	0.003097	0.003081	0.003063	0.003043
0.6	0.002653	0.002641	0.002627	0.002612	0.002595
0.7	0.002113	0.002103	0.002092	0.002080	0.002067
0.8	0.001490	0.001483	0.001476	0.001467	0.001458
0.9	0.000786	0.000782	0.000778	0.000774	0.000769
1.0	0.000000	0.000000	0.000000	0.000000	0.000000

TABLE I (continued)

p=0.7

ζ	τ=0.0	τ=0.1	τ=0.2	τ=0.3	τ=0.4	τ=0.5
0.0	1.111809	1.096786	1.052485	0.980963	0.885583	0.770642
0.1	1.097336	1.082562	1.038969	0.968624	0.874755	0.761600
0.2	1.054415	1.040350	0.998891	0.931942	0.842546	0.734646
0.3	0.984464	0.971575	0.933512	0.871993	0.789738	0.690291
0.4	0.889834	0.878456	0.844866	0.790488	0.717644	0.629352
0.5	0.773549	0.763956	0.735622	0.689697	0.628007	0.552998
0.6	0.639178	0.631545	0.608976	0.572321	0.522956	0.462720
0.7	0.490641	0.485030	0.468433	0.441416	0.404939	0.360240
0.8	0.331982	0.328361	0.317658	0.300232	0.276605	0.247504
0.9	0.167182	0.165441	0.160348	0.152027	0.140702	0.126672
1.0	0.000000	0.000001	0.000000	0.000001	0.000001	0.000001

ζ	τ=0.6	τ=0.7	τ=0.8	τ=0.9	τ=1.0
0.0	0.641209	0.502664	0.360570	0.220110	0.085947
0.1	0.634126	0.497602	0.357499	0.218920	0.086497
0.2	0.612938	0.482387	0.348177	0.215208	0.087878
0.3	0.577852	0.456939	0.332321	0.208457	0.089448
0.4	0.529238	0.421212	0.309444	0.197883	0.090199
0.5	0.467657	0.375169	0.278999	0.182508	0.088854
0.6	0.393874	0.318870	0.240458	0.161292	0.083917
0.7	0.308878	0.252588	0.193388	0.133188	0.073925
0.8	0.213900	0.176822	0.137545	0.097342	0.057359
0.9	0.110394	0.092281	0.073002	0.053037	0.033018
1.0	0.000001	0.000001	0.000001	0.000001	0.000001

TABLE I (continued)

p=1.3

$\mathcal{S}$	τ=0.0	τ=0.1	τ=0.2	τ=0.3	τ=0.4	τ=0.5
0.0	4.229141	4.101032	3.729791	3.152231	2.423257	1.608129
0.1	4.137074	4.014271	3.657845	3.101531	2.396259	1.603611
0.2	3.871483	3.763495	3.448437	2.951887	2.314044	1.585958
0.3	3.462000	3.375258	3.119964	2.710954	2.173744	1.544484
0.4	2.951117	2.888078	2.700212	2.391835	1.973563	1.465373
0.5	2.386238	2.345679	2.222375	2.012825	1.715623	1.336460
0.6	1.812325	1.790145	1.720718	1.596177	1.407881	1.151521
0.7	1.266134	1.256973	1.226373	1.165789	1.064234	0.912470
0.8	0.773705	0.771972	0.764470	0.744444	0.702537	0.629591
0.9	0.349893	0.350812	0.352469	0.351232	0.341960	0.319145
1.0	0.000000	0.000000	0.000000	0.000001	0.000001	0.000001

$\mathcal{S}$	τ=0.6	τ=0.7	τ=0.8	τ=0.9	τ=1.0
0.0	0.774532	-0.014586	-0.706479	-1.262679	-1.661274
0.1	0.788394	0.012294	-0.672171	-1.225719	-1.625234
0.2	0.824618	0.087344	-0.574022	-1.118411	-1.519583
0.3	0.868154	0.194837	-0.425971	-0.951571	-1.351507
0.4	0.897948	0.311373	-0.249787	-0.742752	-1.133416
0.5	0.891838	0.409859	-0.072483	-0.515317	-0.883166
0.6	0.831616	0.464517	0.077254	-0.296582	-0.623484
0.7	0.707445	0.455546	0.173343	-0.114597	-0.380555
0.8	0.519646	0.372806	0.196620	0.005685	-0.181092
0.9	0.278197	0.217254	0.138073	0.046440	-0.048704
1.0	-0.000001	-0.000001	-0.000001	-0.000001	-0.000001

TABLE I (continued)

p=1.9

ξ	τ=0.0	τ=0.1	τ=0.2	τ=0.3	τ=0.4	τ=0.5
0.0	7.358412	7.025445	6.090639	4.719055	3.113719	1.458651
0.1	7.074171	6.775176	5.927620	4.662041	3.147651	1.549865
0.2	6.289392	6.077647	5.457317	4.475939	3.215782	1.788465
0.3	5.178576	5.072835	4.736706	4.130782	3.234348	2.080023
0.4	3.953730	3.938935	3.857039	3.614839	3.112618	2.300747
0.5	2.796747	2.839235	2.927808	2.958599	2.798833	2.341108
0.6	1.822193	1.886921	2.051535	2.231525	2.304685	2.145955
0.7	1.074548	1.135794	1.301378	1.517344	1.696243	1.731928
0.8	0.546849	0.590307	0.712344	0.885820	1.062182	1.173436
0.9	0.203518	0.224698	0.285489	0.376906	0.480609	0.567680
1.0	0.000000	0.000000	0.000000	0.000000	0.000000	0.000001

ξ	τ=0.6	τ=0.7	τ=0.8	τ=0.9	τ=1.0
0.0	-0.106067	-1.476939	-2.569241	-3.312363	-3.663739
0.1	0.007387	-1.366967	-2.477056	-3.242456	-3.615012
0.2	0.322028	-1.051355	-2.204992	-3.031638	-3.464985
0.3	0.762786	-0.574623	-1.770749	-2.679454	-3.204218
0.4	1.216435	-0.015233	-1.213896	-2.195261	-2.823729
0.5	1.555792	0.518538	-0.604556	-1.610103	-2.325643
0.6	1.676274	0.907844	-0.042480	-0.986870	-1.735479
0.7	1.531071	1.056631	0.360719	-0.419789	-1.112252
0.8	1.145349	0.925321	0.514511	-0.016596	-0.547650
0.9	0.600750	0.544603	0.383195	0.134718	-0.147860
1.0	-0.000001	-0.000001	-0.000001	-0.000001	-0.000001

Using the dimensionless variables and parameters defined in Eq. (40), the Fredholm integral equation (38) is

$$\phi(a\delta, a\rho) - \frac{1}{\pi}\int_0^1 \phi(a\delta, a\tau)\, a K(a\tau, a\rho)\, d\tau = F(a\delta, a\tau) \qquad (43)$$

If the ratio of uniform pressure, q, to the constant yield limit, Y, is defined by

$$\gamma = q/Y \qquad (44)$$

the expression for $F(a\delta, a\rho)$ can be written

$$F(a\delta, a\rho) = \frac{2}{\pi}\frac{(1-\nu)}{\mu} Y \begin{cases} \gamma, & \rho < \delta \\ \gamma - \dfrac{\rho}{\sqrt{\rho^2-\delta^2}}(\gamma+1), & \delta < \rho < 1 \end{cases} \qquad (45)$$

It is desirable to avoid the singularity at $\rho = \delta$ in the function $F(a\delta, a\rho)$ when solving the Fredholm equation for $\phi(a\delta, a\rho)$. Both sides of Eq. (43) can be multiplied by $\frac{a}{\pi} K(a\rho, a\tau)$ and integrated with respect to ρ from 0 to 1, yielding

$$Q(a\delta, a\tau) - \frac{1}{\pi}\int_0^1 Q(a\delta, a\rho)\, a K(a\rho, a\tau)\, d\rho = Q_0(a\delta, a\tau) \qquad (46)$$

where

$$Q(a\delta, a\tau) = \frac{1}{\pi}\int_0^1 \phi(a\delta, a\rho)\, a K(a\rho, a\tau)\, d\rho$$

and the function

$$Q_0(a\delta, a\tau) = \frac{1}{\pi}\int_0^1 F(a\delta, a\rho)\, a K(a\rho, a\tau)\, d\rho$$

is finite for all τ.

Since Eq. (46) is an integral equation in $Q(a\delta, a\tau)$ without singularities, its solution (see, for example, Lovitt [27] p. 9) can be found by the method of successive substitution, using for the kernel the values of $aK(a\rho, a\tau)$ calculated from Eq. (42). The recurrence relation

$$Q_n(a\delta, a\tau) = Q_0(a\delta, a\tau) + \frac{1}{\pi}\int_0^1 Q_{n-1}(a\delta, a\rho)\, aK(a\rho, a\tau)\, d\rho \qquad (47)$$

where n=1,2,3,···

will converge rapidly to a solution, $Q(a\delta, a\tau)$, by increasing n until the quantity $|Q_n(a\delta, a\tau) - Q_{n-1}(a\delta, a\tau)|$ is sufficiently small for all τ. The function $\phi(a\delta, a\rho)$ in Eq. (43) can then be found from the relation

$$\phi(a\delta, a\rho) = Q(a\delta, a\rho) + F(a\delta, a\rho) \qquad (48)$$

Matrices, $Q(a\delta, a\rho)$, for values of δ and ρ between 0 and 1 are given in Table II for various combinations of the ratios p and γ. Values for the function $\phi(a\delta, a\rho)$ when the function $F(a\delta, a\rho)$ is non-singular (i.e., when the pressure distribution is uniform over the interval $0 \leq r \leq a$) were tabulated by Uflyand [23] p.204, and agree with those values calculated by Eqs. (47) and (48) for the case

TABLE II

MATRIX OF THE FUNCTION

for p=0.1, γ=0.2, $\frac{(\nu-1)\gamma}{\mu}$=1/520

$Q(a\delta, a\tau) \times 10^3$

τ	δ=0.0	δ=0.2	δ=0.4	δ=0.6	δ=0.8	δ=1.0
0.00	-0.001093	-0.001014	-0.000789	-0.000450	-0.000062	0.000219
0.10	-0.001092	-0.001014	-0.000789	-0.000450	-0.000062	0.000218
0.20	-0.001091	-0.001013	-0.000788	-0.000449	-0.000061	0.000218
0.30	-0.001089	-0.001011	-0.000787	-0.000449	-0.000061	0.000218
0.40	-0.001086	-0.001009	-0.000785	-0.000448	-0.000061	0.000217
0.50	-0.001083	-0.001005	-0.000782	-0.000446	-0.000061	0.000217
0.60	-0.001079	-0.001001	-0.000779	-0.000444	-0.000061	0.000216
0.70	-0.001074	-0.000997	-0.000776	-0.000442	-0.000061	0.000215
0.80	-0.001068	-0.000992	-0.000772	-0.000440	-0.000060	0.000214
0.90	-0.001062	-0.000986	-0.000767	-0.000438	-0.000060	0.000212
1.00	-0.001055	-0.000980	-0.000762	-0.000435	-0.000060	0.000211

TABLE II (continued)

for p=1.0, γ=0.5, $\frac{(1-\nu)Y}{\mu}$ =1/520

$Q(a\delta,a\tau) \times 10^3$

τ	δ=0.0	δ=0.2	δ=0.4	δ=0.6	δ=0.8	δ=1.0
0.00	-0.896370	-0.793194	-0.514062	-0.138042	0.228833	0.448189
0.10	-0.878690	-0.778068	-0.505444	-0.137240	0.223176	0.439348
0.20	-0.826678	-0.733492	-0.479882	-0.134635	0.206652	0.413342
0.30	-0.743348	-0.661837	-0.438266	-0.129694	0.186586	0.371677
0.40	-0.633584	-0.567004	-0.382203	-0.121749	0.147015	0.316795
0.50	-0.503747	-0.454170	-0.314025	-0.110147	0.108508	0.251876
0.60	-0.361335	-0.329578	-0.236871	-0.094542	0.067892	0.180668
0.70	-0.214392	-0.200091	-0.154532	-0.075056	0.027944	0.107196
0.80	-0.070932	-0.072708	-0.071270	-0.052352	-0.008857	0.035466
0.90	0.061719	0.046021	0.008569	-0.027604	-0.040560	-0.030860
1.00	0.177494	0.150521	0.080961	-0.002348	-0.065883	-0.088747

TABLE II (continued)

for $p=1.9$, $\gamma=0.8$, $\frac{(\gamma-1)Y}{\mu}=1/520$

$Q(a\delta, a\tau) \times 10^3$

τ	$\delta=0.0$	$\delta=0.2$	$\delta=0.4$	$\delta=0.6$	$\delta=0.8$	$\delta=1.0$
0.00	-4.768773	-3.872799	-1.669039	0.850840	2.853723	3.814999
0.10	-4.636470	-3.785708	-1.669251	0.785621	2.757440	3.709155
0.20	-4.238643	-3.515146	-1.653893	0.600072	2.471065	3.390897
0.30	-3.590766	-3.052630	-1.587569	0.324949	2.012146	2.872595
0.40	-2.722934	-2.397932	-1.426116	0.009176	1.413245	2.178331
0.50	-1.684685	-1.572380	-1.135189	-0.287122	0.724337	1.347743
0.60	-0.550108	-0.628637	-0.708937	-0.505597	0.012801	0.440089
0.70	0.580241	0.346897	-0.181433	-0.606540	-0.642424	-0.464190
0.80	1.587094	1.243266	0.375891	-0.582338	-1.164495	-1.269672
0.90	2.353671	1.947257	0.872508	-0.459625	-1.497349	-1.882923
1.00	2.796760	2.374305	1.227309	-0.287433	-1.621511	-2.237391

that l =a, i.e., δ =1.

The problem at this point is to use the values computed for $\phi(a\delta, a\delta)$ to solve for the stress distribution at the plane z=0 corresponding to each value of δ. The stress distribution at the plane z=0 is determined by the inverse Hankel transform of Eq. (18)

$$\sigma_{z}\Big|_{z=0} = \frac{\mu}{1-\nu}\int_0^\infty \left[\frac{\xi^2h^2 - \sinh^2 \xi h}{\xi h + \sinh \xi h \cosh \xi h}\right]\xi^2 B_1(\xi) J_0(r\xi)\, d\xi \tag{49}$$

If, as before, the substitutions (21), (25), (27), (29), and (30) are applied to Eq. (49) the stress distribution on the plane of symmetry is given by

$$\sigma_{z}\Big|_{z=0} = \frac{\mu}{1-\nu}\left\{\frac{1}{\pi}\int_0^a \phi(t)\int_0^r K(t,x,a)\frac{dx}{\sqrt{r^2-x^2}}\,dt - \int_0^r \frac{\phi(t)\,dt}{\sqrt{r^2-t^2}}\right\} \tag{50}$$

in the region $0 \leq r < a$, and

$$\sigma_{z}\Big|_{z=0} = \frac{\mu}{1-\nu}\left\{\frac{1}{\sqrt{r^2-a^2}}\int_0^a \phi(t)\,dt - \int_0^a \frac{\phi(t)\,dt}{\sqrt{r^2-t^2}} + \frac{1}{\pi}\int_0^a \phi(t)\int_0^r K(t,x,a)\frac{dx}{\sqrt{r^2-x^2}}\,dt\right\} \tag{51}$$

in the region $r > a$.

The solution to Eq. (50) will, of course, yield the boundary conditions corresponding to the particular plastic zone width assumed. When Eq. (51) is solved for the limiting case when r=a, however, only one choice of plastic zone width will yield stresses finite everywhere.

To solve Eq. (51) it is again convenient to introduce the dimensionless variables and parameters

$$\xi = \frac{x}{a}, \quad \tau = \frac{t}{a}, \quad \delta = \frac{l}{a}, \quad \rho = \frac{r}{a} \tag{52}$$

and substitute for $\phi(t)$, the relation (48)

$$\phi(a\delta, a\tau) = Q(a\delta, a\tau) + F(a\delta, a\tau)$$

Eq. (51) can now be put in the dimensionless form

$$\frac{\sigma_z}{\mu}\bigg|_{z=0} = \frac{1}{1-\nu}\Bigg\{\frac{1}{\sqrt{\rho^2-1}}\int_0^1 [Q(a\delta, a\tau)+F(a\delta, a\tau)]\,d\tau \tag{53}$$

$$-\int_0^1 \frac{[Q(a\delta, a\tau)+F(a\delta, a\tau)]}{\sqrt{\rho^2-\tau^2}}\,d\tau$$

$$+\frac{1}{\pi}\int_0^1 [Q(a\delta, a\tau)+F(a\delta, a\tau)]\int_0^\rho aK(a\tau, a\xi)\,\frac{d\xi}{\sqrt{\rho^2-\xi^2}}\,d\tau\Bigg\}$$

where $Q(a\delta, a\tau)$ and $aK(a\tau, a\xi)$ have been calculated and from Eq. (45)

$$F(a\delta, a\tau) = \frac{2}{\pi}\frac{(1-\nu)}{\mu}\,y\begin{cases} \gamma, & \tau < \delta \\ \gamma - \dfrac{\tau}{\sqrt{\tau^2-\delta^2}}(\gamma+1), & \delta < \tau < 1 \end{cases}$$

The function $F(a\varsigma, a\tau)$ in the first two terms of Eq. (53) can be integrated directly, yielding for the stress

$$\frac{\sigma_z}{\mu}\Big|_{z=0} = \frac{1}{\sqrt{\rho^2-1}}\left\{\frac{2}{\pi}\frac{Y}{\mu}\left[\gamma-(1+\gamma)\sqrt{1-\varsigma^2}\right]+\frac{1}{1-\nu}\int_0^1 Q(a\varsigma,a\tau)\,d\tau\right\} \qquad (54)$$

$$+\frac{2}{\pi}\frac{Y}{\mu}\left[(1+\gamma)\arcsin\sqrt{\frac{1-\varsigma^2}{\rho^2-\varsigma^2}}-\gamma\arcsin(\rho)\right.$$

$$-\frac{1}{1-\nu}\int_0^1\frac{Q(a\varsigma,a\tau)}{\sqrt{\rho^2-\tau^2}}\,d\tau$$

$$+\frac{1}{\pi}\frac{1}{(1-\nu)}\int_0^1\left[Q(a\varsigma,a\tau)+F(a\varsigma,a\tau)\right]\int_0^{\rho}aK(a\tau,a\xi)\frac{d\xi}{\sqrt{\rho^2-\xi^2}}\,d\tau$$

Using the above formula, the stress distribution can be computed for the elastic region where $\rho > 1$ by using numerical quadrature formulae. The stress distributions using Eq. (54) are tabulated in Table III and plotted in Figure 3 for several assumed plastic zone widths. However, in only one case does the particular choice of ς actually correspond to a plastic zone width. For all other choices of ς the stress is either positively or negatively infinite at r=a (i.e., ρ =1.0), thus violating the condition of finiteness of stress.

Only the first term in either Eq. (51) or Eq. (54) is singular for r=a. Thus, the condition of finiteness of stress requires that the numerator of this term is zero. The width of the plastic zone, a-l, can now be determined numerically

TABLE III

STRESS DISTRIBUTIONS CORRESPONDING TO ASSUMED VALUES OF δ

	Stress/Yield Stress, $\sigma_{\bar{x}}/Y$			
r/a	$\delta=.94$	$\delta=.90$	$\delta=.86$	$\delta=.82$
1.00	1.00016	1.00019	1.00021	1.00024
1.02	1.01360	0.60077	0.24021	-0.08203
1.04	0.73483	0.49137	0.26783	0.06230
1.06	0.58920	0.41844	0.25578	0.10284
1.08	0.49467	0.36489	0.23774	0.11629
1.10	0.42690	0.32337	0.21968	0.11894
1.20	0.25004	0.20221	0.15116	0.09922
1.30	0.17030	0.14131	0.10945	0.07630
1.50	0.09193	0.07769	0.06167	0.04469

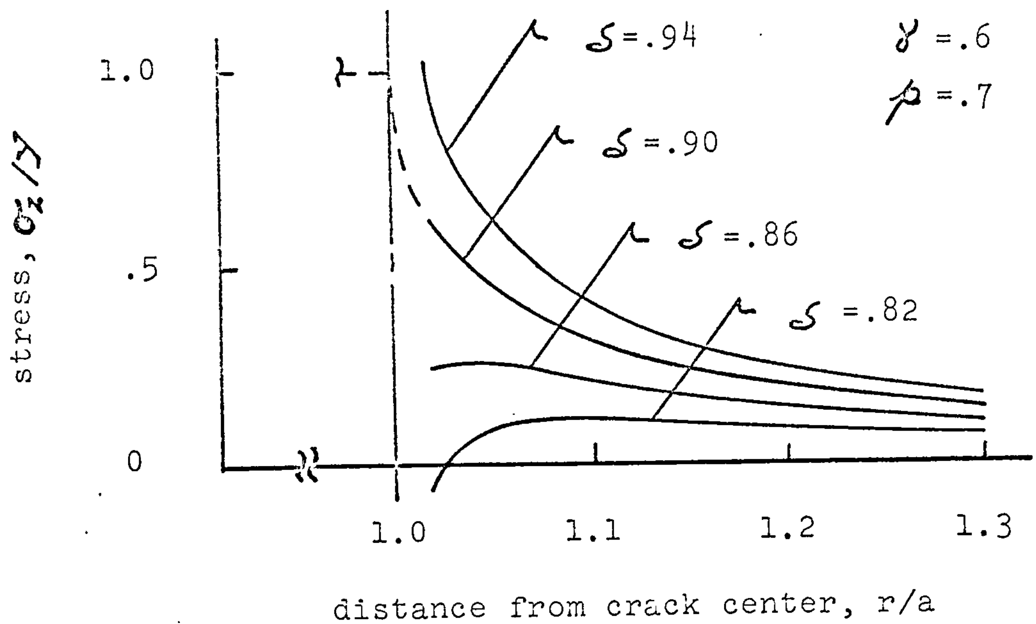

FIGURE 3

STRESS DISTRIBUTION CURVES FOR DETERMINATION OF THE WIDTH OF PLASTIC ZONES by finding that value of $\delta = \frac{l}{a}$ that satisfies the equation

$$\int_0^a \phi(t)\,dt = 0 \tag{55}$$

or what is the same thing

$$\gamma - (\gamma+1)\sqrt{1-\delta^2} + \frac{\pi}{2}\frac{\mu}{(1-\nu)Y}\int_0^1 Q(a\delta, a\tau)\,d\tau = 0 \tag{56}$$

Table IV lists the residues of Eq. (56) for values of δ increased incrementally from 0.5 to 1.0 for various combinations of layer thickness and loading pressure. The width of the plastic zone is taken to be that width corresponding to the residue nearest zero. With a step size equal to .02 for δ, the width of the plastic zone taken from Table IV is found to within 2.0 percent of the radius, a.

For the special case that the ratio, $p = a/h$, is zero (i.e., an infinitely thick layer), $Q(a\delta, a\tau)$ is zero and Eq. (56) reduces to the corresponding equation, for finding the width of the plastic zone around a circular crack in an infinite medium, given by Z. Olesiak and M. Wnuk [21].

$$\lambda - (1+\lambda)\sqrt{1-m^2} = 0 \tag{57}$$

where λ denotes the dimensionless loading, q/Y, and m is the dimensionless ratio of radii, l/a.

TABLE IV

RESIDUES OF EQUATION (56)

	Residue for p=0.7	
l/a	$\gamma=0.4$	$\gamma=0.8$
0.82	-0.37217	-0.14217
0.84	-0.32406	-0.08032
0.86	-0.27269	-0.01427
0.88	-0.21739	0.05682
0.90	-0.15718	0.13423
0.92	-0.09056	0.21988
0.94	-0.01499	0.31705
0.96	0.07454	0.43217
0.98	0.19098	0.58188

	Residue for p=1.9	
l/a	$\gamma=0.4$	$\gamma=0.8$
0.72	-0.57234	-0.12553
0.74	-0.49729	-0.02904
0.76	-0.42132	0.06863
0.78	-0.34442	0.16751
0.80	-0.26653	0.26765
0.82	-0.18757	0.36918
0.84	-0.10734	0.47233
0.86	-0.02557	0.57746
0.88	0.05820	0.68517
0.90	0.14469	0.79638
0.92	0.23515	0.91268
0.94	0.33174	1.03687
0.96	0.43898	1.17475
0.98	0.56897	1.34188

5. Computation of Stress and Displacement

By using the values of $Q(a\delta, a\tau)$ and $F(a\delta, a\tau)$ corresponding to the calculated plastic zone width, Eq. (54) for the stress distribution in the elastic region on the plane of symmetry, reduces to

$$\frac{\sigma_z}{\mu} = \frac{2}{\pi}\frac{Y}{\mu}\left[(1+\gamma)\arcsin\sqrt{\frac{1-\delta^2}{\rho^2-\delta^2}} - \gamma\arcsin(\rho)\right]$$
$$- \frac{1}{1-\nu}\int_0^1 \frac{Q(a\tau)}{\sqrt{\rho^2-\tau^2}}\,d\tau$$
$$+ \frac{1}{\pi}\frac{1}{(1-\nu)}\int_0^1\left[Q(a\tau)+F(a\tau)\right]\int_0^\rho aK(a\tau, a\rho)\frac{d\rho}{\sqrt{\rho^2-\rho^2}}\,d\tau \tag{58}$$

The stress distribution can be calculated using methods of numerical quadrature for any desired layer thickness, loading condition, and material constants.

The displacement of the crack faces can be found from the inverse Hankel transform of Eq. (17)

$$w_{z=0} = \int_0^\infty \xi B_1(\xi) J_0(r\xi)\,d\xi \tag{59}$$

By substituting for $\xi^2 B_1(\xi)$ from Eq. (21) and interchanging the order of integration, Eq. (59) can be written

$$w = \int_0^a \phi(t)\int_0^\infty \frac{1}{\xi}(\cos\xi t - \cos\xi a) J_0(r\xi)\,d\xi\,dt \tag{60}$$

After applying the relation (26)

$$\int_0^\infty \frac{(\cos\xi t - \cos\xi a)}{\xi} J_0(r\xi)\,d\xi$$

$$= \begin{cases} 0, \quad r > a \\ \cosh^{-1}\frac{a}{r} = \log(a+\sqrt{a^2-r^2}) - \log(r)\,, \quad t < r < a \\ \cosh^{-1}\frac{a}{r} - \cosh^{-1}\frac{t}{r} = \\ \log(a+\sqrt{a^2-r^2}) - \log(t+\sqrt{t^2-r^2}), \quad r < t < a \end{cases}$$

the formula for displacement of the crack surface becomes

$$w = \log(a+\sqrt{a^2-r^2})\int_0^a \phi(t)\,dt - \log(r)\int_0^r \phi(t)\,dt \qquad (61)$$
$$- \int_r^a \phi(t)\log(t+\sqrt{t^2-r^2})\,dt$$

In dimensionless form, Eq. (61) is

$$w/a = \log(1+\sqrt{1-\rho^2})\int_0^1 \phi(a\tau)\,d\tau \qquad (62)$$
$$- \log(\rho)\int_0^\rho \phi(a\tau)\,d\tau$$
$$- \int_\rho^1 \phi(a\tau)\log(\tau+\sqrt{\tau^2-\rho^2})\,d\tau$$

After replacing $\phi(a\tau)$ by the function $F(a\tau)$ plus the computed values of $Q(a\tau)$, Eq. (53) can be solved by numerical quadrature for the displacement of the crack surface corresponding to any assumed plastic zone width. The actual displacement, however, is computed using $\phi(a\tau)$ corresponding to that particular plastic zone width that satisfies Eq. (55). Therefore the equation for the actual displacement simplifies to

$$w/a = -\log(\rho)\int_0^{\rho}\phi(a\tau)\,d\tau - \int_{\rho}^{1}\phi(a\tau)\log(\tau+\sqrt{\tau^2-\rho^2})\,d\tau \tag{63}$$

The displacements of the crack surfaces can now be computed using Eq. (63) for any desired layer thickness, loading pressure, and material constants.

CHAPTER III

NUMERICAL EXAMPLES

Eq. (56) for plastic zone width, Eq. (58) for stress, and Eq. (63) for displacement were solved by numerical quadrature for various combinations of loading pressure to yield limit ratio, γ, and crack radius to layer thickness ratio, p.

The trapezoidal rule was used for performing all numerical integrations where no singularities were present in the functions to be integrated. All other numerical integrations involved the integration of the product of a function such as $Q(a\delta, a\tau)$, and a singular, but integrable function such as $1/\sqrt{\rho^2-\tau^2}$. In this case, since the tabulated function $Q(a\delta, a\tau)$ is reasonably flat in the interval $0 \leq \tau \leq 1$ and the integral of $1/\sqrt{\rho^2-\tau^2}$ is well known, the method of numerical integration indicated by C. Lanczos [28], p. 54, can be employed.

For example, the integration

$$f(\delta,\tau) = \int_0^{\rho} Q(\delta,\tau)\frac{d\tau}{\sqrt{\rho^2-\tau^2}}, \quad 0 < \rho \leq 1$$

can be approximated with a high degree of accuracy by the summation

$$f(\delta,\tau) = \sum_{i=1}^{\rho/\Delta} \frac{Q(\delta,\tau_{i-1}) + Q(\delta,\tau_i)}{2}\left[\arcsin\frac{i\Delta}{\rho} - \arcsin\frac{(i-1)\Delta}{\rho}\right]$$

where

Δ is the step size,

$$\int \frac{d\tau}{\sqrt{\rho^2-\tau^2}} = \arcsin\frac{\tau}{\rho}$$

$Q(\delta, \tau_i)$ are values of the function

$Q(a\delta, a\tau)$ tabulated for values

of τ , $0 \leq \tau \leq 1$

All calculations for the examples given in this chapter were based on material constants typical for mild steel,

shear modulus, μ = 11.5×10^6 psi

Poisson's ratio, ν = 1/3

yield limit, Y = 33,000 psi

The results of these calculations are tabulated in Tables V through X in the Appendix and are plotted in Figures 4 through 11 in this chapter.

Figure 4 shows that either an increase in the loading pressure, q, or a decrease in the plate thickness, h, will cause the plastic zone to increase in width. It also shows that for the ratio, h/a equal to ten or greater, the plastic zone width can be determined by Eq. (57) as if the crack were in an infinite body; it is not necessary to consider the thickness of the layer. Figures 5 and 6 also give the relationship between the plastic zone width, the loading

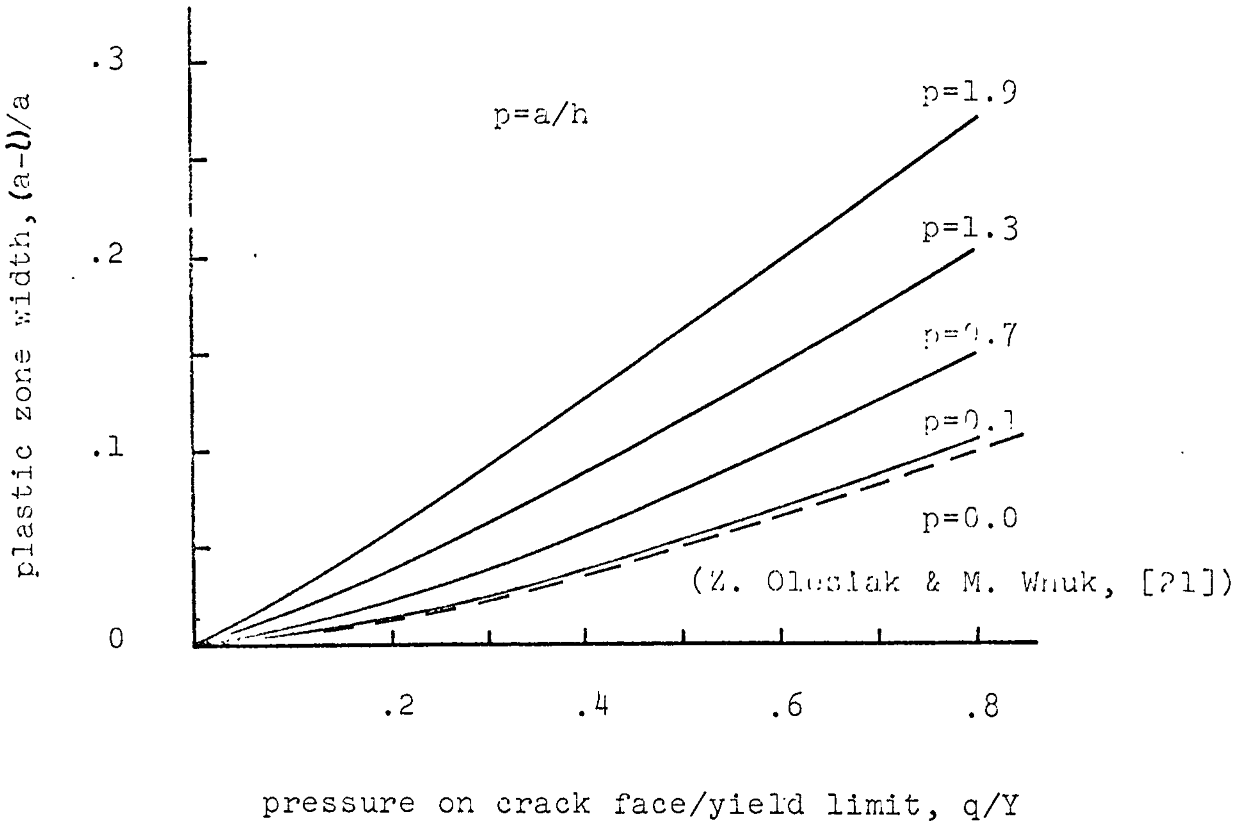

FIGURE 4

VARIATION OF PLASTIC ZONE WIDTH WITH PRESSURE FOR SPECIFIED LAYER THICKNESSES[4]

---

[4] For tabulated data, see Table V, p. 63.

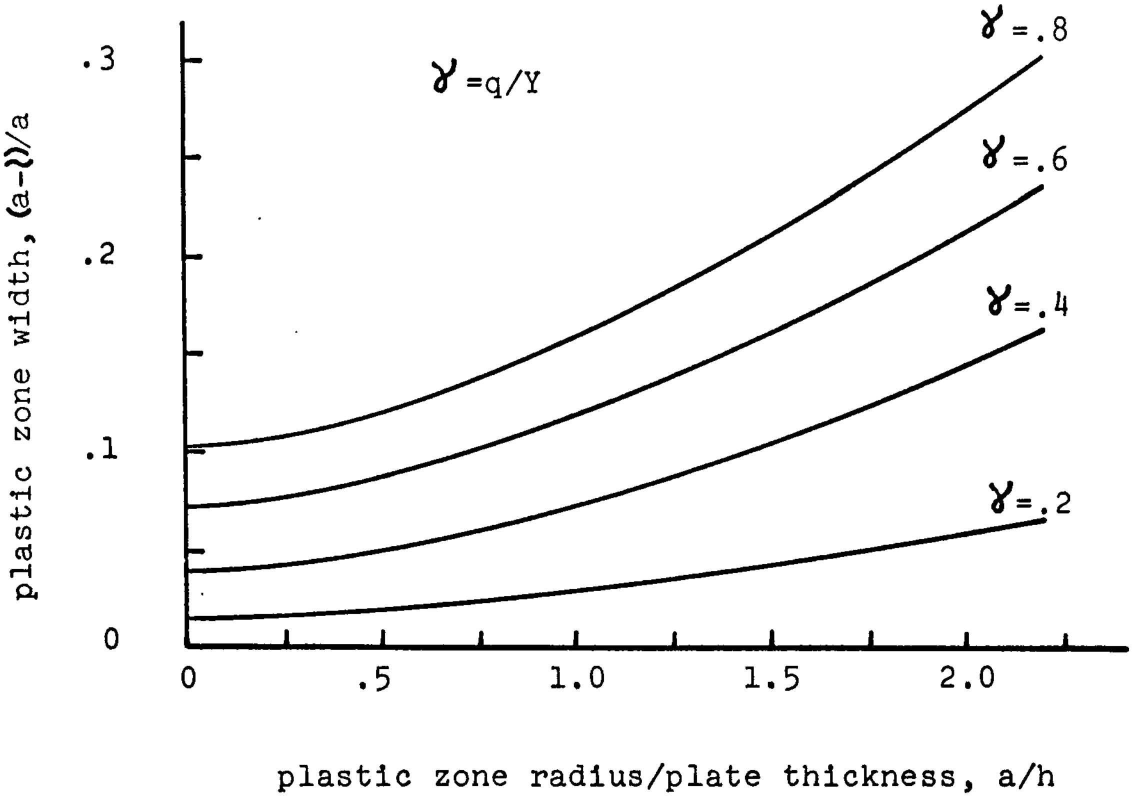

FIGURE 5

VARIATION OF PLASTIC ZONE WIDTH WITH LAYER THICKNESS FOR SPECIFIED LOADING PRESSURES[5]

---

[5]For tabulated data, see Table V, p. 63.

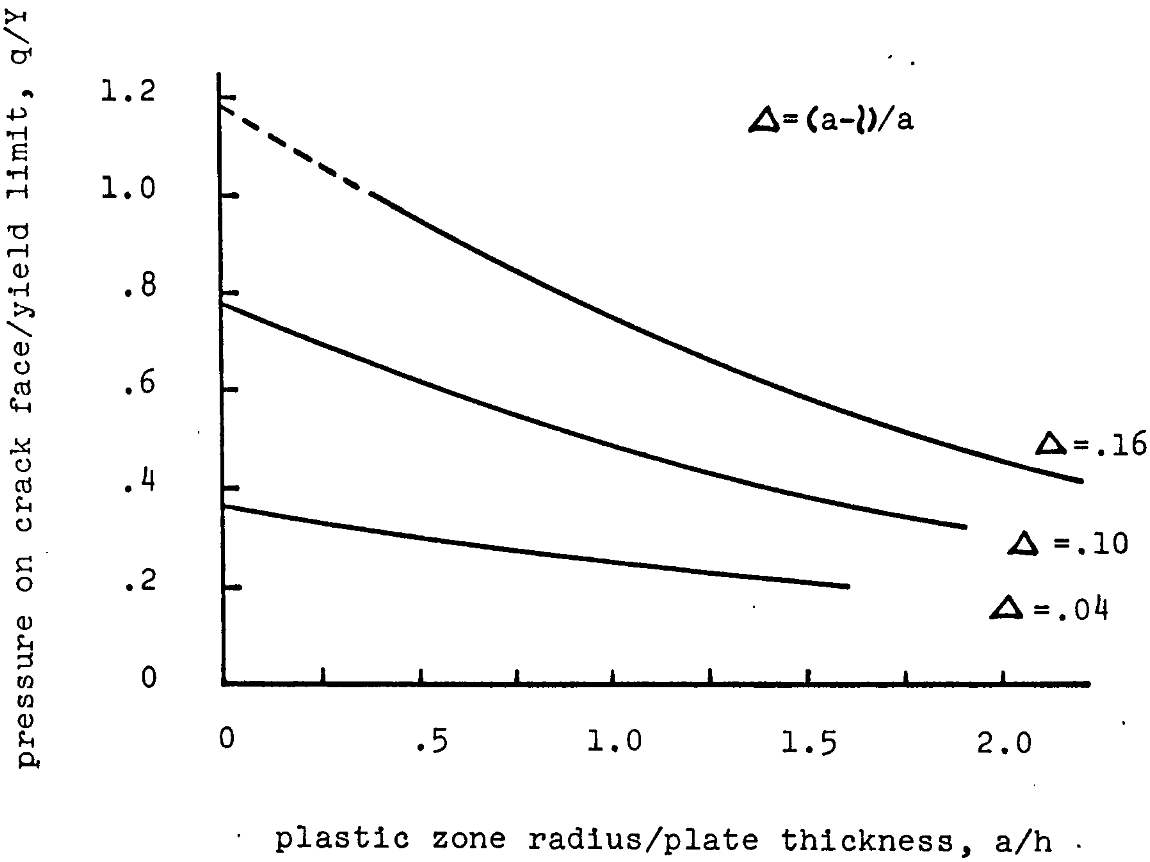

FIGURE 6

PAIRS OF LOADING PRESSURES AND LAYER THICKNESSES PRODUCING EQUAL PLASTIC ZONE WIDTHS[6]

---

[6] For tabulated data, see Table V, p.63.

pressure, and the layer thickness. Any three of the parameters λ, a, p, and q/Y may be selected arbitrarily; but, the fourth must satisfy the relationships plotted in these Figures.

Figure 7 represents the variation of the dimensionless stress σ_z/μ with the dimensionless distance r/a from the center of symmetry for different values of the loading ratio q/Y. Only the normal stress on the plane of symmetry has been computed here; however, once the width of the plastic zone has been obtained, one can find the stress and displacement at any point in the layer by numerically evaluating the inverse Hankel transforms of Eqs. (10) and (12).

The family of curves shown in Figure 8 represents the distribution of dimensionless normal stress, σ_z/μ for different layer thicknesses when the loading pressure is held constant. In very thin layers, the stress near the plastic zone is somewhat higher than that in thicker layers; however, since the thinner layer has a wider plastic zone, the same loading pressure is distributed over a smaller area and the stress at distant points is lower.

The displacements of the crack surfaces produced by the applied pressures are shown in Figures 9 through 11. The general shape of these curves near the crack tips demonstrates the result predicted by G. I. Barenblatt (Barenblatt [11] considered an annulus of forces of cohesion and not a

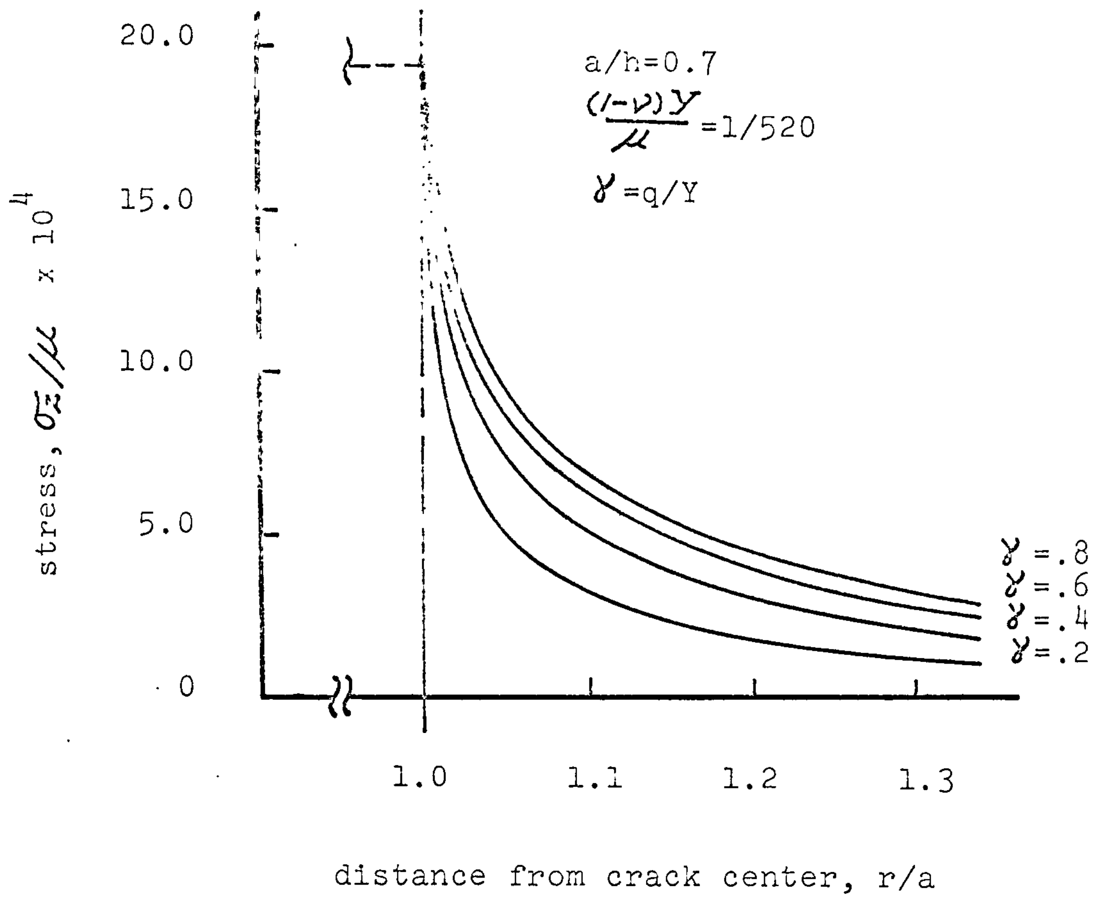

FIGURE 7

VARIATION OF STRESS DISTRIBUTION AT PLANE OF SYMMETRY WITH LOADING PRESSURE[7]

---

[7]For tabulated data, see Table VI, p. 64.

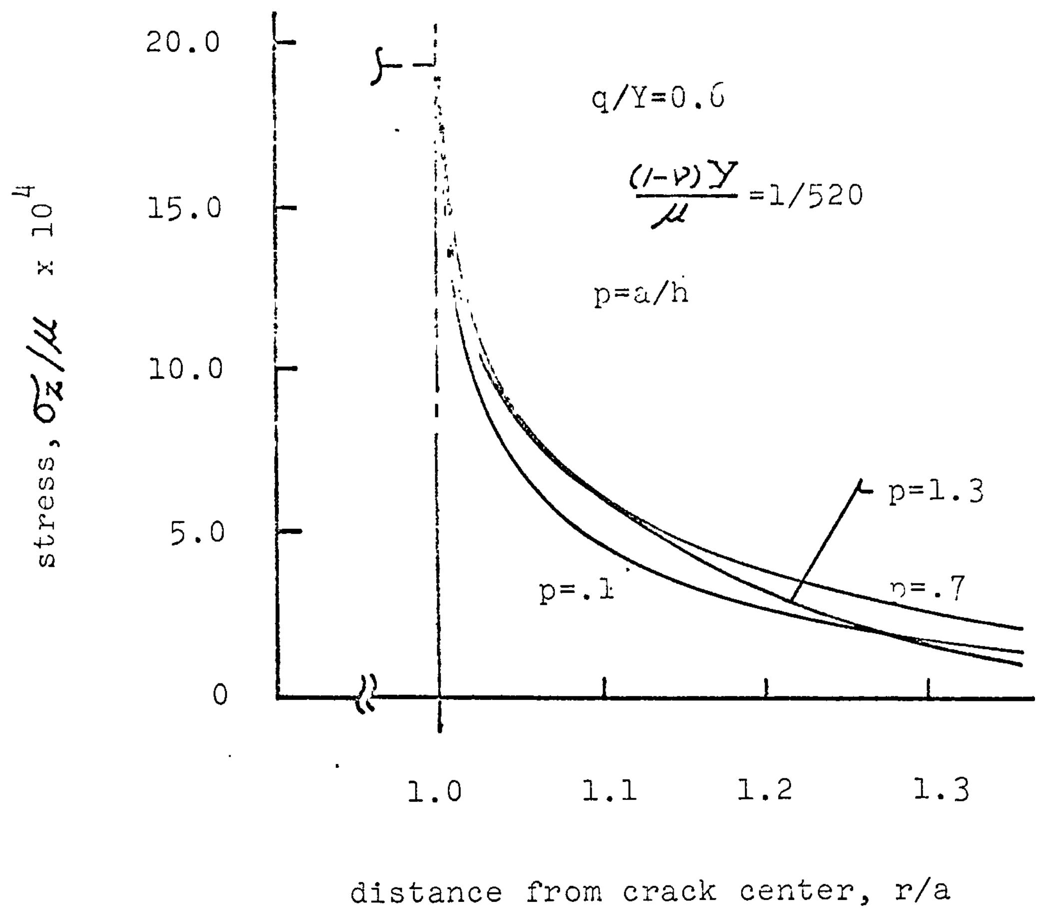

FIGURE 8

VARIATION OF STRESS DISTRIBUTION AT PLANE OF SYMMETRY WITH LAYER THICKNESS[8]

---

[8]For tabulated data, see Table VII, p. 65.

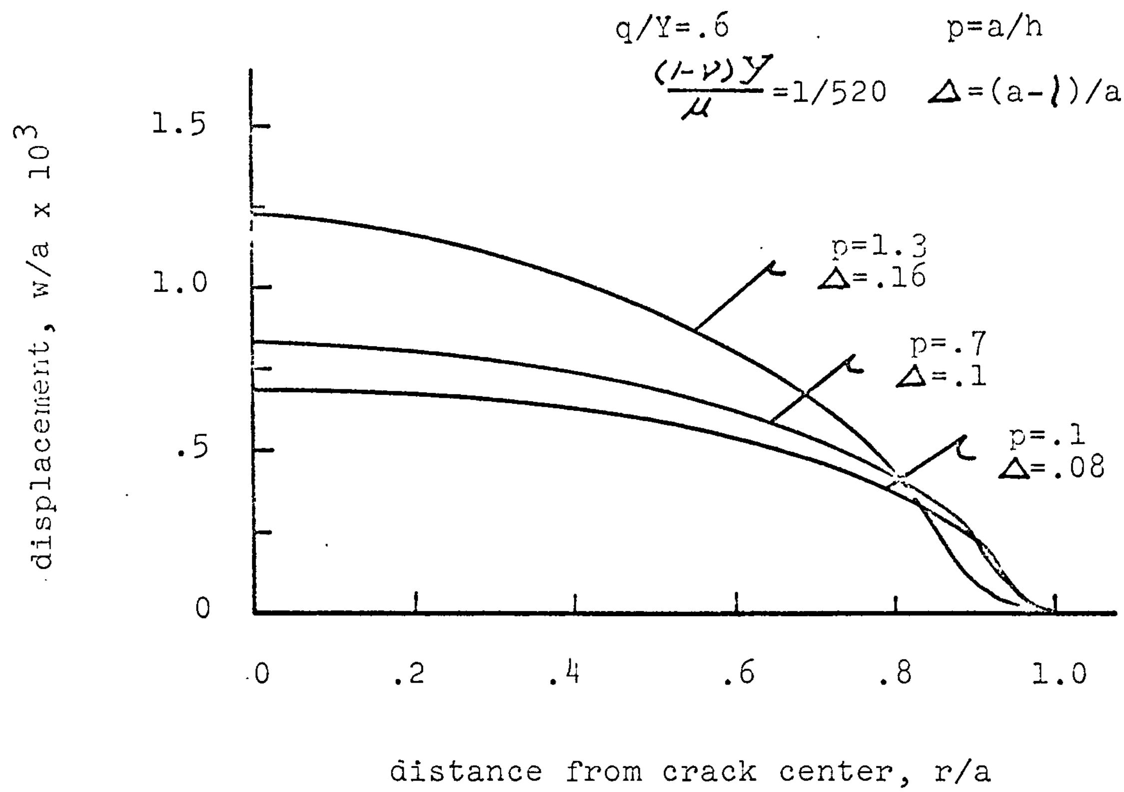

FIGURE 9

VARIATION OF CRACK SURFACE DISPLACEMENT WITH LAYER THICKNESS FOR SPECIFIED LOADING PRESSURE[9]

---

[9]For tabulated data, see Table VIII, p. 66.

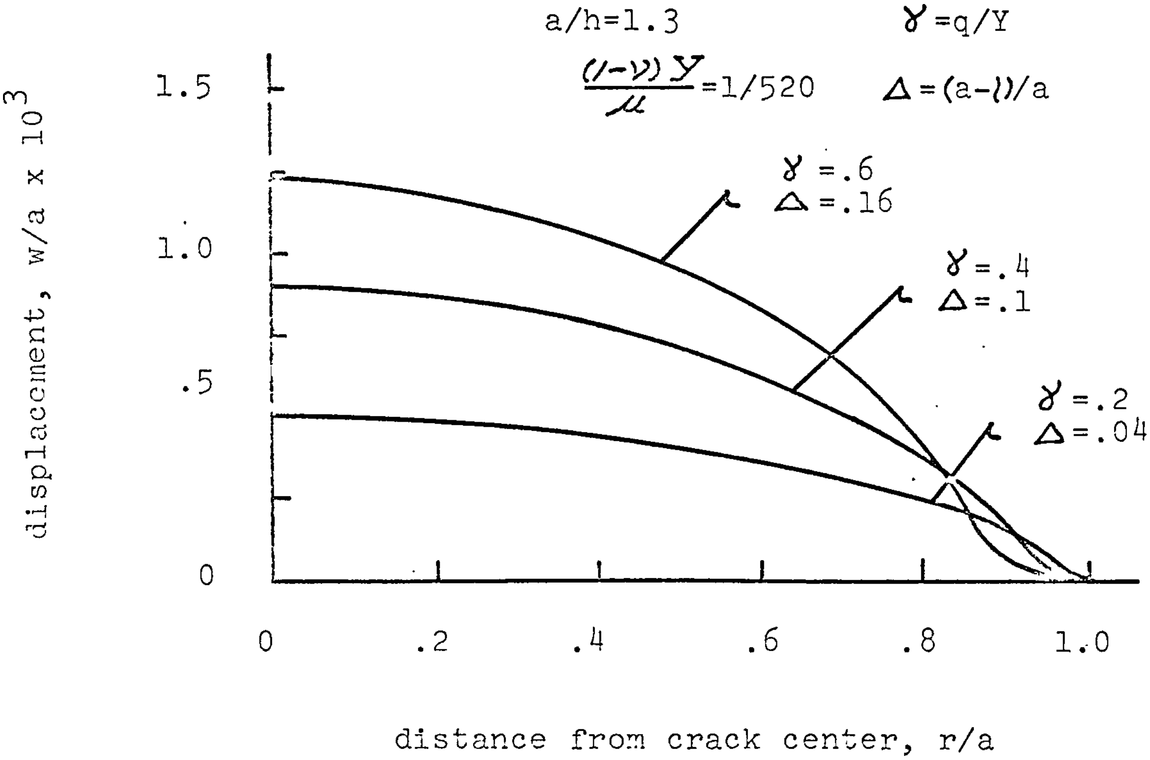

FIGURE 10

VARIATION OF CRACK SURFACE DISPLACEMENT WITH LOADING PRESSURE FOR SPECIFIED LAYER THICKNESS[10]

---

[10] For tabulated data, see Table IX, p. 67.

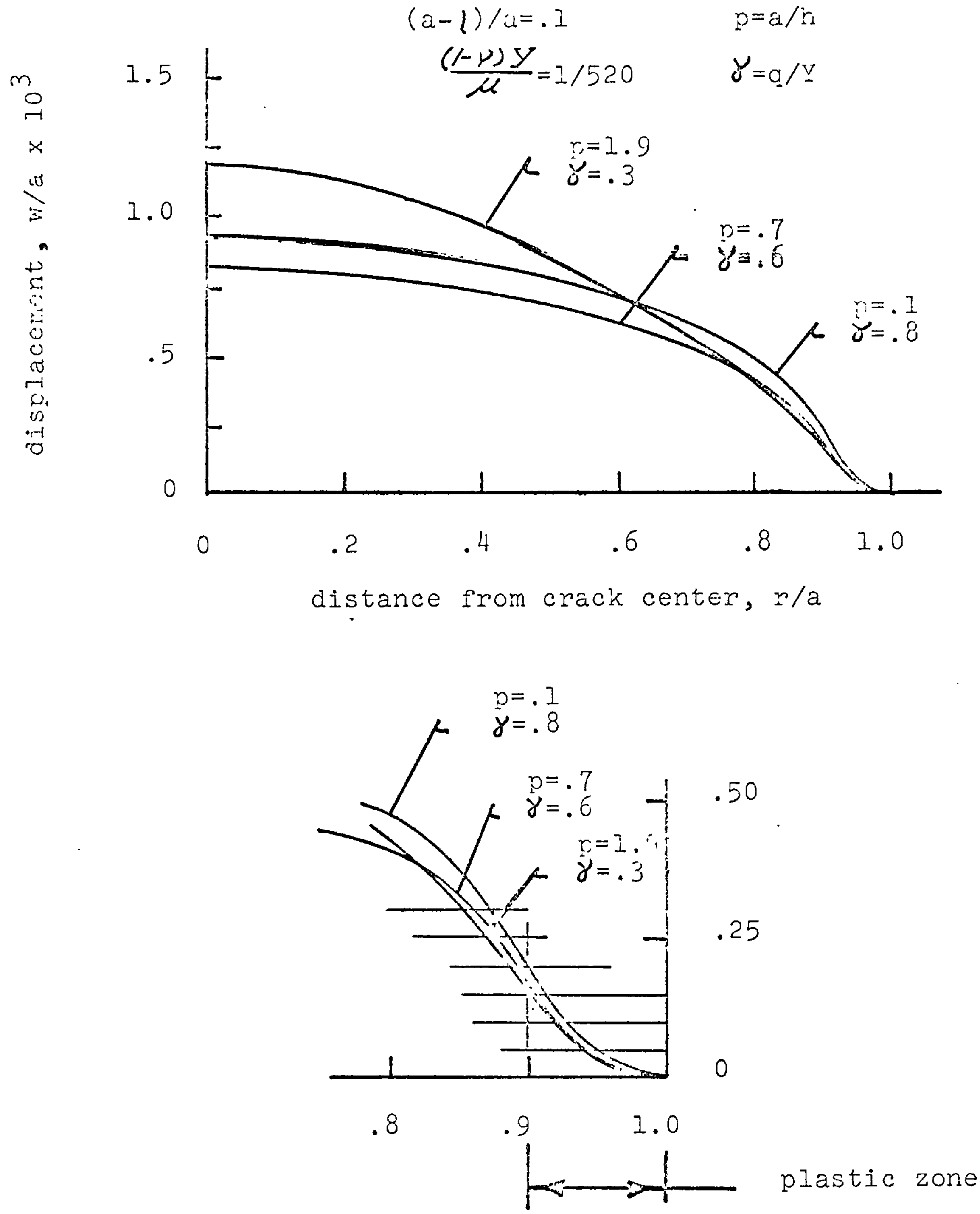

FIGURE 11

VARIATION OF CRACK SURFACE DISPLACEMENT
WITH LOAD AND LAYER THICKNESS FOR
SPECIFIED PLASTIC ZONE WIDTH[11]

---

[11]For tabulated data, see Table X, p. 68.

plastic zone) that the condition of finiteness of stress corresponds to smooth closing of the crack surfaces.

The displacement curves obtained can be useful in determining whether or not the assumptions that the displacements are small and that the plastically deformed material is confined to a very thin region at the crack tips are justified. In this regard, one can compare the displacements of the crack surface and the thickness of the plastic zone to certain characteristic dimensions of the problem.

When compared to either the crack diameter or the plate thickness, the maximum opening of the crack is smaller by several orders of magnitude. Therefore, for all examples considered here the assumption of small displacements is well justified. Only for cases in which the ratios of layer thickness to crack diameter are much smaller than those considered here might the displacements be so large as to be cause for concern.

For purposes of establishing a criteria for determining the conditions required for the crack to extend, it is generally agreed that the thickness of the plastic zone should be small. For example, when the crack expands there is a layer of plastically deformed material on the elastic boundary of the crack. When this layer is thick the Orowan modification [13] to the Griffith energy criteria of fracture [9] will not apply because the elastic energy release rate due to extension of the crack is calculated on the assumption that the volume of plastically deformed material is so small that the material may be considered to be elastic throughout. Furthermore, if there were a very thick layer of plastically deformed material on the elastic boundary of the crack, (the same boundary on which, in this problem, the loading pressure is applied) the actual stress field near the crack tips would be somewhat different than that calculated here.

When compared with the width of the plastic zone, the maximum thickness of the plastic zone is smaller by an order of magnitude of three. However, as shown in Figures 9, 10, and 11, the maximum crack opening is approximately five times the maximum plastic zone thickness. The highest ratios (approximately seven) correspond to cases where the loading pressure is small and the layer is thin. In no case is the ratio less than four. The answer to whether or not a ratio of four, or even seven, is too small to permit one to define the conditions required for crack extension would require an investigation into the effects of plastic zone thickness on the particular crack extension criteria applied.

CHAPTER IV

CONCLUSIONS

The problem of finding the stresses and displacements in a layer of elastic-perfectly plastic material containing a penny-shaped crack has been solved by reducing the problem to one within the theory of elasticity of finding the stresses and displacements in a half-layer of elastic material with the proper boundary conditions.

The widths of the annulus of yielded material around the crack have been calculated for various layer thicknesses and loading pressures based on the condition of finiteness of stress. It was observed that for layer thickness of at least ten times the crack diameter, the layer can be considered an infinite body.

Utilizing the computed values of plastic zone width, the stresses and displacements on the plane of symmetry have been calculated. The stress field at the elastic-plastic interface is continuous. The shape of the crack faces at the tip of the crack verifies that the elastic boundary of the crack is not rounded at the tip as observed in solutions for ideally elastic bodies containing cracks, but closes smoothly into a cusp corresponding to the condition of finiteness of stress.

The maximum displacements were found to be small when compared to certain characteristic dimensions of the problem, thus satisfying the theory of elasticity requirement of small strain. The maximum thickness of the plastic zone was found to be approximately one-fifth the maximum crack opening.

BIBLIOGRAPHY

1. Irwin, G. R. _Fracture Mechanics_, Pergamon Press, New York, 1960.

2. Barenblatt, G. I. "Mathematical Theory of Equilibrium Cracks in Brittle Fracture," _Advances in Applied Mechanics_, VII (1962) 55.

3. Paris, P. C., and G. C. Sih. "Stress Analysis of Cracks," _Fracture Toughness Testing and its Applications_, ASTM Special Technical Publication No. 381, Philadelphia (1965) 30.

4. Sneddon, I. N. _Crack Problems in the Theory of Elasticity_, North Carolina State College, Raleigh, 1961.

5. Inglis, C. E. "Stresses in a Plate Due to the Presence of Cracks and Sharp Corners," _Trans. Inst. Nav. Arch._, 55 (1913) 219.

6. Muskhelishvili, N. I. "Sur l'Integration de l'Equation Biharmonique," _Izvestiya Ross. Akad. Nauk_, 13 (1919) 663.

7. Westergaard, H. M. "Stresses at a Crack, Size of the Crack, and the Bending of Reinforced Concrete," _J. Americ. Concrete Inst._, 5, No. 2 (1933) 93.

8. Sneddon, I. N. "The Distribution of Stress in the Neighborhood of a Crack in an Elastic Solid," _Proc. Roy. Soc._, A 187 (1946) 229.

9. Griffith, A. A. "The Phenomenon of Rupture and Flow in Solids," _Phil. Trans. Roy. Soc._ A 221 (1919) 163.

10. Zheltov, Yu. P., and S. A. Khristianovitch. "On the Mechanism of Hydraulic Fracture of an Oil-Bearing Stratum," _Izvestiya AN SSSR, OTN_, No. 5 (1955) 3. (in Russian)

11. Barenblatt, G. I. "On Conditions of Finiteness in Mechanics of Continua. Static Problems in the Theory of Elasticity," _Prikl. Matem. i Mechan._, 24 (1960) 316.

12. Irwin, G. R. "Fracture Dynamics," _Fracturing of Metals_, ASM, Cleveland, Ohio (1948) 147.

13. Orowan, E. O. "Energy Criteria of Fracture," Welding Journal, Res. Suppl., 34 (1955) 157S.

14. Gerberich, W. W. "Plastic Strains and Energy Density in Cracked Plates, I. Experimental Technique and Results," Proc. SESA, 21 (1964) 335.

15. Swedlow, J. L., and W. W. Gerberich. "Plastic Strains and Energy Density in Cracked Plates, II. Comparison with Elastic Theory," Proc. SESA, 21 (1964) 345.

16. Frost, N. E., and D. S. Dugdale. "The Propagation of Fracture Cracks in Sheet Specimens," J. Mech. Physics of Solids, 6 (1958) 92.

17. Dugdale, D. S. "Yielding of Steel Sheets Containing Slits," J. Mech. Physics of Solids, 8 (1960) 100.

18. Rice, J. R. "Stresses Due to a Sharp Notch in a Work-Hardening Elastic-Plastic Material Loaded by Longitudinal Shear," J. Appl. Mech., 34 No. 2 (1967) 287.

19. McClintock, F. A., and G. R. Irwin. "Plasticity Aspects of Fracture Mechanics," Fracture Toughness Testing and its Applications, ASTM Special Technical Publication No. 381, Philadelphia (1965) 84.

20. Goodier, J. N., and F. A. Field. "Plastic Energy Dissipation in Crack Propagation," Fracture of Solids, edited by D. C. Drucker and J. J. Gilman, New York (1963) 103.

21. Olesiak, Z., and M. Wnuk. "Length of Plastic Zones for Penny-Shaped Cracks," Bul. L'Acad. Pol. Sciences, Serie Techn. XIII, No. 8 (1965) 445.

22. Olesiak, Z., and M. Wnuk. "Plastic Energy Dissipation Due to a Penny-Shaped Crack," submitted for publication in the Journal of Engineering Fracture Mechanics.

23. Uflyand, Ya. S. Integral Transforms in Problems of the Theory of Elasticity, The Academy of Sciences of the U.S.S.R., Moscow and Leningrad (1963) 201-06.

24. Keer, L. M. "Class of Non-Symmetrical Punch and Crack Problems," Quart. J. Mech. and Appl. Math., 17 Pt. 4 (1964) 424.

25. Olesiak, Z., and I. N. Sneddon. "The Distribution of Thermal Stress in an Infinite Elastic Solid Containing a Penny-Shaped Crack," *Arch. Rational Mech. and Anal.*, 4 No. 3 (1960) 238.

26. Erdelyi, A. *Tables of Integral Transforms*, II, McGraw-Hill, New York, 1954.

27. Lovitt, W. V. *Linear Integral Equations*, Dover Publications, New York, 1950.

28. Lanczos, C. *Linear Differential Operators*, Van Nostrand, London, 1961.

APPENDIX

TABLE V

WIDTHS OF PLASTIC ZONES CORRESPONDING TO PAIRS OF PLATE THICKNESSES AND LOADING PRESSURES

	Width of Plastic Zone, $(a-\ell)/a$							
q/Y \ a/h	0.1	0.4	0.7	1.0	1.3	1.6	1.9	2.2
0.2	0.02	0.02	0.02	0.02	0.04	0.04	0.06	0.06
0.3	0.02	0.04	0.04	0.04	0.06	0.08	0.10	0.12
0.4	0.04	0.04	0.06	0.08	0.10	0.12	0.14	0.16
0.5	0.06	0.06	0.08	0.10	0.12	0.14	0.16	0.18
0.6	0.08	0.08	0.10	0.12	0.16	0.18	0.20	0.22
0.7	0.08	0.10	0.12	0.14	0.18	0.20	0.22	0.24
0.8	0.10	0.12	0.14	0.16	0.20	0.24	0.26	0.28
0.9	0.12	0.12	0.16	0.20	0.22	0.26	0.28	0.30

TABLE VI

VARIATION OF STRESS DISTRIBUTION AT THE PLANE OF SYMMETRY WITH LOADING PRESSURE

$a/h=0.7 \quad (1-\nu)Y/\mu = 1/520$

$\sigma_z/\mu \times 10^4$

r/a	q/Y=.2	q/Y=.4	q/Y=.6	q/Y=.8
1.00	19.2317	19.2329	19.2344	19.2361
1.02	7.8453	10.1855	11.5534	12.0675
1.04	5.5971	8.0273	9.4495	10.1322
1.06	4.4068	6.6679	8.0469	8.7803
1.08	3.6477	5.7110	7.0171	7.7563
1.10	3.1140	4.9928	6.2187	6.9435
1.20	1.1772	3.0085	3.8887	4.4692
1.30	1.1929	2.0696	2.7176	3.1642
1.50	0.6386	1.1248	1.4941	1.7565

TABLE VII

VARIATION OF STRESS DISTRIBUTION AT THE PLANE OF SYMMETRY WITH LAYER THICKNESS

$q/Y=0.6$ $(1-\nu)Y/\mu=1/520$

$\sigma_z/\mu \times 10^4$

r/a	a/h=.1	a/h=.7	a/h=1.3
1.00	19.2306	19.2344	19.2343
1.02	9.7847	11.5534	11.0276
1.04	7.7975	9.4495	9.3864
1.06	6.4661	8.0469	8.0991
1.08	5.5022	7.0171	7.0621
1.10	4.7680	6.2187	6.2013
1.20	2.7287	3.8887	3.3673
1.30	1.7997	2.7176	1.7715
1.50	0.9567	1.4993	0.4629

TABLE VIII

VARIATION OF CRACK SURFACE DISPLACEMENT WITH LAYER THICKNESS FOR SPECIFIED LOADING PRESSURE

$q/Y=0.6$, $(1-\nu)Y/\mu=1/520$, $\Delta=(a-l)/a$

$w/a \times 10^3$

r/a	a/h=0.1 Δ =.08	a/h=0.7 Δ =.10	a/h=1.3 Δ =.16	a/h=1.9 Δ =.20
0.00	0.694697	0.819363	1.21173	1.94186
0.10	0.692698	0.816568	1.20423	1.92426
0.14	0.688634	0.811245	1.19243	1.89894
0.18	0.683388	0.804367	1.17717	1.86616
0.22	0.676880	0.795842	1.15836	1.82593
0.26	0.669052	0.785610	1.13600	1.77839
0.30	0.659840	0.773604	1.11009	1.72375
0.34	0.649184	0.759759	1.08064	1.66229
0.38	0.637003	0.743994	1.04765	1.59430
0.42	0.623206	0.726208	1.01113	1.52010
0.46	0.607679	0.706280	0.971016	1.44000
0.50	0.590286	0.684060	0.927242	1.35427
0.54	0.570853	0.659351	0.879660	1.26311
0.58	0.549163	0.631904	0.828022	1.16661
0.62	0.524932	0.601386	0.771931	1.06458
0.66	0.497787	0.567348	0.710740	0.956421
0.70	0.467218	0.529154	0.643374	0.840687
0.74	0.432489	0.485865	0.567939	0.714005
0.78	0.392482	0.435990	0.480654	0.566811
0.82	0.345331	0.376872	0.371609	0.343768
0.86	0.287409	0.302757	0.185538	0.214817
0.90	0.209222	0.173394	0.091512	0.120243
0.94	0.057166	0.052668	0.031149	0.051454
0.98	0.017486	0.018308	0.009709	0.020806
1.00	0.000000	0.000000	0.000000	0.000000

TABLE IX

VARIATION OF CRACK SURFACE DISPLACEMENT WITH LOADING PRESSURE FOR SPECIFIED LAYER THICKNESS

$a/h=1.3$, $(1-\nu)Y/\mu=1/520$, $\Delta=(a-l)/a$

$w/a \times 10^3$

r/a	q/Y=0.2 Δ=.04	q/Y=0.4 Δ=.10	q/Y=0.6 Δ=.16	q/Y=0.8 Δ=.20
0.00	0.493997	0.895289	1.21173	1.52686
0.10	0.491335	0.890130	1.20423	1.51703
0.14	0.487023	0.881891	1.19243	1.50167
0.18	0.481453	0.871245	1.17717	1.48179
0.22	0.474602	0.858142	1.15836	1.45729
0.26	0.466470	0.842577	1.13600	1.42813
0.30	0.457065	0.824560	1.11009	1.39430
0.34	0.446404	0.804116	1.08064	1.35580
0.38	0.434502	0.781263	1.04765	1.31262
0.42	0.421375	0.756017	1.01113	1.26471
0.46	0.407035	0.728382	0.971016	1.21196
0.50	0.391490	0.698343	0.927242	1.15421
0.54	0.374737	0.665858	0.879660	1.09117
0.58	0.356759	0.630841	0.828022	1.02238
0.62	0.337517	0.593141	0.771931	0.947076
0.66	0.316939	0.552511	0.710740	0.864011
0.70	0.294906	0.508548	0.643374	0.770989
0.74	0.271222	0.460591	0.567939	0.663658
0.78	0.245568	0.407503	0.480654	0.530715
0.82	0.217403	0.347150	0.371609	0.309384
0.86	0.185740	0.274712	0.185538	0.190332
0.90	0.148518	0.155248	0.091512	0.105841
0.94	0.099881	0.045080	0.031149	0.045586
0.98	0.022268	0.014695	0.009709	0.018568
1.00	0.000000	0.000000	0.000000	0.000000

TABLE X

VARIATION OF CRACK SURFACE DISPLACEMENT WITH LOAD AND LAYER THICKNESS FOR SPECIFIED PLASTIC ZONE WIDTH

$(a-\ell)/a=.90, \quad (1-\nu)Y/\mu = 1/520$

$w/a \times 10^3$

r/a	a/h=0.1 q/Y=0.8	a/h=0.7 q/Y=0.6	a/h=1.3 q/Y=0.4	a/h=1.9 q/Y=0.3
0.00	0.915869	0.819363	0.895289	1.17105
0.10	0.913142	0.816568	0.890130	1.16157
0.14	0.907665	0.811245	0.881891	1.14763
0.18	0.900587	0.804367	0.871245	1.12960
0.22	0.891803	0.795842	0.858142	1.10746
0.26	0.881234	0.785610	0.842577	1.08128
0.30	0.868793	0.773604	0.824560	1.05118
0.34	0.854393	0.759759	0.804116	1.01731
0.38	0.837925	0.743994	0.781263	0.979817
0.42	0.819259	0.726208	0.756017	0.938904
0.46	0.798237	0.706280	0.728382	0.894761
0.50	0.774664	0.684060	0.698343	0.847589
0.54	0.748297	0.659351	0.665858	0.797581
0.58	0.718823	0.631904	0.630841	0.744907
0.62	0.685835	0.601386	0.593141	0.689691
0.66	0.648789	0.567348	0.552511	0.631982
0.70	0.606927	0.529154	0.508548	0.571690
0.74	0.559141	0.485865	0.460591	0.508490
0.78	0.503686	0.435990	0.407503	0.441616
0.82	0.437492	0.376872	0.347150	0.369377
0.86	0.353966	0.302757	0.274712	0.287586
0.90	0.207641	0.173394	0.155248	0.164100
0.94	0.070021	0.052668	0.045080	0.051567
0.98	0.026951	0.018308	0.014695	0.018003
1.00	0.000000	0.000000	0.000000	0.000000